CHAPTER 8

OPTIMAL MANEUVERS OF RIGID SPACECRAFT

8.1 INTRODUCTORY REMARKS

This chapter is concerned with application of the methods of Chapters 3, 4, 6, 7 to three specific classes of rigid (or near-rigid) spacecraft maneuvers. The emphasis here is upon illustrating methodology for solving the TPBVP's arising in specific applications and, especially, the interplay between problem formulation, physical insights, and the degree of difficulty encountered in determination of the optimal maneuvers. The three maneuver problems discussed in Sections 8.2, 8.3, 8.4 are of increasing generality and dimensionality; the first two are examples of large nonlinear maneuvers successfully performed by spacecraft presently in orbit.

8.2 MINIMUM-TIME MAGNETIC ATTITUDE MANEUVERS

8.2.1 Background

Several investigators (refs. 1-13) have developed and applied control laws for generating magnetic torques for (1) precession/nutation damping, (2) momentum dumping (from reaction wheels), and (3) large-angle maneuvers. Spacecraft that are presently operational utilize (or have utilized) all three types of magnetic torque strategies. Apparently none of the large-angle magnetic torque maneuvers of existing spacecraft (prior to the NOVA-1 spacecraft launch in May 1981) has been of the minimum time variety, although typical magnetic manevuers require hours or occasionally, even days to complete. The method discussed below was developed for NOVA-1 and was successfully performed. Perhaps the anticipation of a complicated nonlinear two-point boundary-value problem (TPBVP) has deterred earlier effort in this direction.

Tossman (ref. 1) formulated the necessary conditions for time-optimal magnetic control for a spin-stabilized spacecraft, under the assumption that the earth's magnetic field is a nonrotating dipole. Tossman also introduced an approximate form for a switching function, (for the current in an electromagnet aligned with the spin axis), which limits the practical applicability of his developments. Tossman's work, however, led to an elegantly simple one-dimensional TPBVP approximate optimal maneuver.

The present developments are motivated by the work of Tossman but we retain the generality of using state-of-the-art orbit integrators and magnetic field models. We develop below a time-optimal "slow maneuver formulation" which shares (with Tossman's work) the most attractive feature of a bounded one-dimensional search to solve the resulting TPBVP.

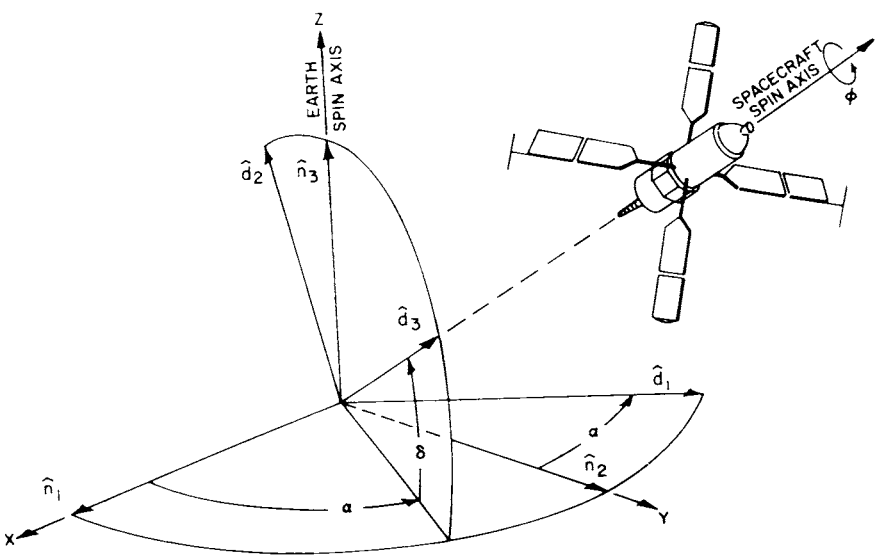

Figure 8.1 Geometry for Magnetic Maneuvers of a Spin Stabilized Symmetric Spacecraft

8.2.2 Kinematics and Dynamics

Consider the angular motion of a spin-stabilized symmetric spacecraft (Fig. 8.1). A despun, dextral coordinate frame $\{\hat{\mathbf{d}}\}$ is associated with the vehicle such that $\hat{\mathbf{d}}_3$ is along the axis of symmetry (right ascension α, delination δ) and $\hat{\mathbf{d}}_1$ lies in the inertial $(\hat{\mathbf{n}}_1, \hat{\mathbf{n}}_2)$ plane as shown.

The spacecraft (S) angular velocity is then

$$\omega_S = \dot{\alpha}\hat{\mathbf{n}}_3 - \dot{\delta}\hat{\mathbf{d}}_1 + \dot{\phi}\hat{\mathbf{d}}_3 \tag{8.1}$$

where $\dot{\phi}$ is the vehicle spin velocity relative to the $\{\hat{\mathbf{d}}\}$ frame, and $(\cdot) \equiv d/dt(\ )$.

The angular velocity of the despun frame (D) is clearly

$$\omega_D = \omega_S - \dot{\phi}\hat{\mathbf{d}}_3 = \dot{\alpha}\hat{\mathbf{n}}_3 - \dot{\delta}\hat{\mathbf{d}}_1 \tag{8.2}$$

For subsequent use, orthogonal components of ω_S and ω_D are taken along the $\{\hat{\mathbf{d}}\}$ basis vectors as

$$\omega_S = \omega_1\hat{\mathbf{d}}_1 + \omega_2\hat{\mathbf{d}}_2 + \omega_3\hat{\mathbf{d}}_3 \quad , \quad \omega_D = \Omega_1\hat{\mathbf{d}}_1 + \Omega_2\hat{\mathbf{d}}_2 + \Omega_3\hat{\mathbf{d}}_3 \tag{8.3}$$

where

$$\omega_1 = \Omega_1 = -\dot{\delta} \quad , \quad \omega_2 = \Omega_2 = \dot{\alpha}\cos\delta \quad , \quad \omega_3 = \Omega_3 + \dot{\phi}$$

and

$$\Omega_3 = \dot{\alpha}\sin\delta$$

The equations of motion follow from (see Ch. 3,4).

$$\text{torque} = d/dt(\text{angular momentum})_N \tag{8.4a}$$

or with $\{\hat{\mathbf{d}}\}$ components

$$\sum_{i=1}^{3} L_i\hat{\mathbf{d}}_i = \frac{d}{dt}\sum_{i=1}^{3} I_i\omega_i\hat{\mathbf{d}}_i\Big)_D + \sum_{j=1}^{3}\Omega_j\hat{\mathbf{d}}_j \times \left[\sum_{i=1}^{3} I_i\omega_i\hat{\mathbf{d}}_i\right] \tag{8.4b}$$

where $d/dt\ (*)_R$ is the time derivative of $(*)$ as seen from frame R, $A(\equiv I_1 = I_2)$ is the transverse centroidal moment of inertia and $C(\equiv I_3 > I_1)$ is the spin axis centroidal moment of inertia. Carrying out the algebra implied in Eq. 8.4b and equating components yields the scalar equations of motion

$$L_1 = -A\ddot{\delta} + (C - A)\dot{\alpha}^2\sin\delta\cos\delta + (C\dot{\phi})\dot{\alpha}\cos\delta$$

$$L_2 = A\ddot{\alpha}\cos\delta + C\dot{\alpha}\dot{\delta}\sin\delta + (C\dot{\phi})\dot{\delta} - 2A\dot{\alpha}\dot{\delta}\sin\delta \qquad (8.5)$$

$$L_3 = C\ddot{\alpha}\sin\delta + C\dot{\alpha}\dot{\delta}\cos\delta + C\ddot{\phi}$$

For spin-stabilized satellites, the spin momentum terms (multiplied by $H_3 \equiv C\dot{\phi}$) generally dominate Eq. 8.5. Under the "slow maneuver" assumption, one can often approximate the right side of Eq. 8.5 by

$$L_1 \cong H_3\dot{\alpha}\cos\delta \quad , \quad L_2 \cong H_3\dot{\delta} \quad , \quad L_3 \cong \dot{H}_3 \qquad (8.6)$$

from which we obtain the widely used approximate rates for slewing of the spin axis

$$\dot{\alpha} \cong L_1/H_3\cos\delta \quad , \quad \dot{\delta} \cong L_2/H_3 \qquad (8.7)$$

Equations 8.7 can be developed by taking an alternative, more physically appealing viewpoint. Spin stabilized spacecraft usually have passive nutation dampers, such as a ring damper normal to the spin axis, which serves to damp nutations rapidly; in the case of the NOVA spacecraft (ref. 13), the time constant is a few minutes. Thus, the spin axis will align with the angular momentum vector quickly, in the absence of external torques. In the presence of a small external torque, the angular momentum vector will vary slowly. In the magnetic torquing cases under consideration, the angular momentum vector changes direction about 5° to 10° per hour, thus it is reasonable to expect the more rapid nutation decay to result in the spin axis remaining very nearly aligned with the instantaneous angular momentum vector.

If the spin axis is assumed exactly colinear with the angular momentum vector, the problem reduces to precessing the angular momentum vector

$$\mathbf{H} \cong (H_3)\hat{\mathbf{d}}_3$$

and we have

$$\mathbf{L} = \frac{d}{dt}(\mathbf{H})_N = \frac{d}{dt}(\mathbf{H})_D + \boldsymbol{\omega}_D \times \mathbf{H}$$

which immediately gives Eqs. 8.6.

Thus Eq. 8.7 can also be derived by assuming that the spin axis always remains aligned with the instantaneous angular momentum vector, so an alternate

interpretation of the slow maneuver assumption is that the nutation motion about the angular momentum vector is always of negligible amplitude. Solutions based upon integrating $(\alpha,\delta,\phi,\dot{\alpha},\dot{\delta},\dot{\phi})$ from Eq. 8.5 (upon including a detailed damper model for the coupling torques and forces) typically oscillate with small amplitude (for well-damped, spin-stabilized satellites) about the (α,δ) solution based upon Eqs. 8.7. Additional terms are required, of course, to account for the specific effects of a particular damper design.

The magnetic torque vector in Eq. 8.7 is given

$$\mathbf{L} = \mathbf{M} \times \mathbf{B} \tag{8.8}$$

where

$$\mathbf{M} = pM\mathbf{d}_3 \tag{8.9}$$

is the spacecraft dipole moment with constant magnitude M and polarity $p(-1,0,1)$, and

$$\mathbf{B} = \sum_{i=1}^{3} B_i \hat{\mathbf{d}}_i \tag{8.10}$$

is the geomagnetic field vector with $\{\hat{\mathbf{d}}\}$ components

$$\begin{Bmatrix} B_1 \\ B_2 \\ B_3 \end{Bmatrix} = \begin{bmatrix} -\sin\alpha & \cos\alpha & 0 \\ -\sin\delta\cos\alpha & -\sin\delta\sin\alpha & \cos\delta \\ \cos\delta\cos\alpha & \cos\delta\sin\alpha & \sin\delta \end{bmatrix} [R(\theta(t),\Phi(t),\lambda(t))] \begin{Bmatrix} B_1 \\ B_2 \\ B_3 \end{Bmatrix} \tag{8.11a}$$

where

$$[R(\theta,\Phi,\lambda)] = \begin{bmatrix} \cos\theta & -\sin\theta & 0 \\ \sin\theta & \cos\theta & 0 \\ 0 & 0 & 1 \end{bmatrix} \begin{bmatrix} -\sin\Phi\cos\lambda & -\sin\lambda & -\cos\Phi\cos\lambda \\ -\sin\Phi\sin\lambda & \cos\lambda & -\cos\Phi\sin\lambda \\ \cos\Phi & 0 & -\sin\Phi \end{bmatrix} \tag{8.11b}$$

projects geomagnetic earth-fixed components of the magnetic field into earth-centered, nonrotating rectangular components, and the down, east, north (B_1, B_2, B_3) geomagnetic field vector is given by the spherical harmonic expansions:

$$\begin{Bmatrix} B_3 \\ B_2 \\ B_3 \end{Bmatrix} = \sum_{n=1}^{N} \frac{1}{r^{n+2}} \quad \frac{1}{\cos\Phi} \begin{Bmatrix} \sum_{m=0}^{n} \frac{dP_n^m(\sin\Phi)}{d\Phi} [G_n^m \cos\lambda + H_n^m \sin m\lambda] \\ \sum_{m=1}^{n} m P_n^m(\sin\Phi)[G_n^m \sin m\lambda - H_n^m \cos m\lambda] \\ -(n+1) \sum_{m=0}^{n} P_n^m(\sin\Phi)[G_n^m \cos m\lambda + H_n^m \sin m\lambda] \end{Bmatrix} \quad (8.12)$$

G_n^m, H_n^m are harmonic coefficients (ref. 14), $P_n^m(\sin\Phi)$ are associated Legendre functions. Observe that

$$\begin{Bmatrix} x_e \\ y_e \\ z_e \end{Bmatrix} = \begin{bmatrix} \cos\theta & \sin\theta & 0 \\ -\sin\theta & \cos\theta & 0 \\ 0 & 0 & 1 \end{bmatrix} \begin{Bmatrix} x \\ y \\ z \end{Bmatrix} \quad (8.13)$$

are the equatorial components of the earth-fixed rectangular position vector of the spacecraft, $\{x,y,z\}^T$ is the instantaneous spacecraft rectangular position vector (from an orbit integration) in a recent equatorial nonrotating coordinate system, so the following transformations yield the spherical (geographic) coordinates

$$\begin{aligned} r &= [x^2 + y^2 + z^2]^{1/2} && \text{radial distance to satellite} \\ \lambda &= \tan^{-1}(y_e/x_e) && \text{geographic east longitude} \\ \Phi &= \sin^{-1}(z/r) && \text{geographic north latitude} \end{aligned} \quad (8.14)$$

Thus, from Eqs. 8.11, the $\{\hat{\mathbf{d}}\}$ components of the geomagnetic field have the functional dependence

$$B_i = \text{function}(\alpha,\delta,t) \quad , \quad i = 1,2,3 \quad (8.15)$$

for specified initial conditions on the orbital motion.

Upon carrying out the substitution of Eqs. 8.9 and 8.10, into Eq. 8.8 we obtain

$$\begin{aligned} L_1 &= pMB_2 = \text{function}(\alpha,\delta,p,t) \\ L_2 &= pMB_1 = \text{function}(\alpha,\delta,p,t) \quad , \quad L_3 = 0 \end{aligned} \quad (8.16)$$

and substituting Eq. 8.16 into Eq. 8.7, we find that slow maneuvers are

governed by the pair of equations

$$\dot{\alpha} = pf_1(\alpha,\delta,t) \quad , \quad \dot{\delta} = pf_2(\alpha,\delta,t) \tag{8.17}$$

where

$$f_1 = m\beta_2/\cos\delta \quad , \quad f_2 = m\beta_1 \quad , \quad m = M/H_3 = \text{const}$$

8.2.3 Optimal Control Formulation

The following developments represent a nonlinear generalization of the linear bang-bang control problem considered in Section 6.5.

We seek to minimize maneuver time = $\int_{t_o}^{t_f} dt$ subject to the requirement that the terminal states are specified

$$\alpha(t_o) = \alpha_o \quad , \quad \delta(t_o) = \delta_o \tag{8.18a}$$

$$\alpha(t_f) = \alpha_f \quad , \quad \delta(t_f) = \delta_f \tag{8.18b}$$

and the trajectory is given by the solution of Eq. 8.17 with the control variable constraint that the polarity satisfies

$$|p(t)| \leq 1 \tag{8.19}$$

In preparing to apply Pontryagin's Principle, (Sections 6.2 and 6.3) we introduce the Hamiltonian functional

$$H = 1 + p(\lambda_1 f_1 + \lambda_2 f_2) \tag{8.20}$$

where λ_1 and λ_2 are co-state variables. Pontryagin's necessary conditions require, in addition to Eqs. (8.17-8.19) that the co-state variables satisfy the adjoint system of differential equations

$$\begin{aligned} \dot{\lambda}_1 &= -\frac{\partial H}{\partial \alpha} = -p\frac{\partial f_1}{\partial \alpha}\lambda_1 + \frac{\partial f_2}{\partial \alpha}\lambda_2 \\ \dot{\lambda}_2 &= -\frac{\partial H}{\partial \delta} = -p\frac{\partial f_1}{\partial \delta}\lambda_1 + \frac{\partial f_2}{\partial \delta}\lambda_2 \end{aligned} \tag{8.21}$$

and the control polarity p(t) is determined, subject to Eq. (8.19), to minimize $H(p(t))$ of Eq. 8.20; this yields the "polarity switching function"

$$p(t) = -\text{sign}[\lambda_1 f_1 + \lambda_2 f_2] \tag{8.22}$$

It is evident, since Eqs. 8.21 and 8.22 contain the λ's linearly, and they do not appear explicitly elsewhere, that a linear scaling of the λ's by a positive constant is immaterial; in other words, *the λ's do not have a unique magnitude.*

Therefore, we are free to arbitrarily constrain the λ's magnitude; we adopt the implicit scaling constraint that the initial costates lie on the unit circle.

$$\lambda_1^2(t_o) + \lambda_2^2(t_o) = 1$$

Strictly speaking, imposing this condition is inconsistent with the transversality necessary condition $H(t_f) = 0$, i.e., Eq. (6.41), for control problems having free final time. However, since extremizing $C\int_{t_o}^{t_f} dt$ is equivalent to extremizing $\int_{t_o}^{t_f} dt$ for C, an unspecified positive constant, then a Hamiltonian $H = C + p(\lambda_1 f_1 + \lambda_2 f_2)$ can be introduced (with exactly the same resulting co-state equations, Eq. 8.21, and switching function, Eq. 8.22). Since an infinity of C values can be chosen, the $\lambda_1^2(t_o) + \lambda_2^2(t_o) = 1$ condition can be introduced since it merely chooses implicitly one of these possible normalizations. If desired, the implicitly specified value of C is simply determined from $H(t_f) = 0$ as $C = [-p(\lambda_1 f_1 + \lambda_2 f_2)]_{t_f}$.

Accordingly, we restrict the initial costates to lie on the unit circle and introduce an initial phase angle γ_o such that

$$\lambda_1(t_o) = \cos\gamma_o \quad , \quad \lambda_2(t_o) = \sin\gamma_o \quad (0 \leq \gamma_o < 360°) \tag{8.23}$$

Sweeping γ_o through 0 to 360° determines a complete family of initial co-states. Each choice on γ_o generates a minimum time trajectory $[\alpha(t), \delta(t)]$ from integration of Eqs. 8.17 and 8.21 with initial conditions of Eqs. 8.18a and 8.23, the optimum polarity switches being given by Eq. 8.22. Recall the linear problem in Section 6.5, we were able to infer that, at most, one control switch occurred along each optimal trajectory. Due to the nonlinearity of Eqs. 8.17, 8.21, 8.22, it is impossible to obtain such insight on the problem at

hand. However, we have been able to reduce the number of free parameters to one (namely γ_o), thus choosing trial values γ_{o_i} $\{0 \leq \gamma_{o_i} < 360°\}$ will generate the family of minimum time trajectories to all reachable end states. For each trial value on the initial co-state phase γ_{o_i}, it is necessary to search along the trajectory for the time of closest approach [wherein $\alpha(t)_i$, $\delta(t)_i$ most nearly coincides with the desired (α_f,δ_f)]. A candidate local extremal is obtained for each γ_{o_i} which generates a time-optimal trajectory passing within, for example, 0.5 deg of (α_f,δ_f). Due to small amplitude, time-varying geomagnetic harmonics, and the present state of knowledge of the best-fitting static geomagnetic field approximation, we believe it is not physically realistic to discuss magnetic control for tolerances much less than 0.5°. Due to the sharp precessional discontinuities at each control switch time, numerical search schemes are complicated by numerous local minima in the miss distance. Alternatively through the use of interactive graphics, we have found an attractive way to reliably and efficiently circumvent this apparent difficulty. Using this interactive approach, optimal solutions can be routinely (and globally) determined in 15 minutes of real time. The minimum time maneuver is not always unique, but the ease with which the extermal field map can be generated and displayed allows confident selection of the global minimum time maneuver (ref. 13).

For convenient reference, the minimum time-optimal maneuver necessary conditions are collected below in back substitution form, including the partial derivatives required in Eqs. 8.21.

$$\left.\begin{aligned} &\dot{\alpha} = pf_1(t,\alpha,\delta) \quad , \quad \dot{\delta} = pf_2(t,\alpha,\delta) \\ &\dot{\lambda}_1 = -p\frac{\partial f_1}{\partial \alpha}\lambda_1 + \frac{\partial f_2}{\partial \alpha}\lambda_2 \quad , \quad \dot{\lambda}_2 = -p\frac{\partial f_1}{\partial \delta}\lambda_1 + \frac{\partial f_2}{\partial \delta}\lambda_2 \\ &p(t) = -\text{sign}[\lambda_1 f_1 + \lambda_2 f_2] \end{aligned}\right\} \qquad (8.24)$$

where

$$f_1 = -m\beta_2/\cos\delta \quad , \quad f_2 = m\beta_1 \quad , \quad m = M/H_3 \quad , \quad H_3 = C\dot{\phi} = \text{constant}$$

$$\left.\begin{aligned} \frac{\partial f_1}{\partial \alpha} &= -m\,\frac{\partial \beta_2}{\partial \alpha}\left(\frac{1}{\cos\alpha}\right) \quad , \quad \frac{\partial f_1}{\partial \delta} = -m\left(\frac{\partial \beta_2}{\partial \delta} - \beta_2 \tan\delta\right)\left(\frac{1}{\cos\delta}\right) \\ \frac{\partial f_2}{\partial \alpha} &= m\,\frac{\partial \beta_1}{\partial \alpha} \quad , \qquad\qquad \frac{\partial f_2}{\partial \delta} = m\,\frac{\partial \beta_1}{\partial \delta} \end{aligned}\right\} \qquad (8.25a)$$

and $\{\beta_1,\beta_2,\beta_3\}$ are the $\{\hat{\mathbf{d}}\}$ components of the geomagnetic field vector which are functions of $\{r(t), \lambda(t), \Phi(t), \alpha, \delta, B_1, B_2, B_3\}$, as in Eqs. 8.11, $\{B_1,B_2,B_3\}$ is the geomagnetic field vector with down, east, north components, computed via a user-prescribed model as a function of $\{\Phi(t), \lambda(t), r(t)\}$, for example, Eq. 8.12, where

$$\begin{aligned} \Phi(t) &= \sin^{-1}(z(t)/r(t)) \\ \lambda(t) &= \tan^{-1}(y_e(t)/x_e(t)) \\ r(t) &= [x^2(t) + y^2(t) + z^2(t)]^{1/2} \end{aligned} \qquad (8.25b)$$

The earth-fixed coordinates of the spacecraft orbital position are given by Eq. 8.13 where $\{x(t), y(t), z(t)\}$ are satellite rectangular coordinates (nonrotating, equatorial) obtained from the solution of the user-prescribed orbital equations of motion,

$$\theta(t) = \theta_{ref} + \omega_e(t - t_{ref}) \text{ , the sideral time of Greenwich,} \qquad (8.25c)$$

and ω_e is the sideral angular rate of Earth's rotation, and θ_{ref} is the sideral angle of Greenwich at time t_{ref}

$$\frac{\partial}{\partial \alpha}\begin{Bmatrix}\beta_1\\ \beta_2\\ \beta_3\end{Bmatrix} = \begin{bmatrix} -\sin\alpha & -\sin\alpha & 0 \\ \sin\delta\sin\alpha & -\sin\delta\cos\alpha & 0 \\ -\cos\delta\sin\alpha & \cos\delta\cos\alpha & 0 \end{bmatrix} [R(\theta,\Phi,\lambda)] \begin{Bmatrix}B_1\\ B_2\\ B_3\end{Bmatrix} \qquad (8.25d)$$

$$\frac{\partial}{\partial \delta}\begin{Bmatrix}\beta_1\\ \beta_2\\ \beta_3\end{Bmatrix} = \begin{bmatrix} 0 & 0 & 0 \\ -\cos\delta\cos\alpha & -\cos\delta\sin\alpha & -\sin\delta \\ -\sin\delta\cos\alpha & -\sin\delta\sin\alpha & \cos\delta \end{bmatrix} [R(\theta,\Phi,\lambda)] \begin{Bmatrix}B_1\\ B_2\\ B_3\end{Bmatrix} \qquad (8.25e)$$

and $[R(\theta(t), \Phi(t), \lambda(t))]$ is given by Eq. 8.11b.

8.2.4 Example Calculations of NOVA Optimal Maneuvers

In solution of the two-point boundary-value problems, it is convenient to use a modified inertial reference frame. This modified inertial frame $\{\hat{n}^*\}$ (Fig. 8.2) is associated with the initial and desired pointing directions, we define $\{\hat{n}^*\}$ as follows:

$$\begin{aligned}
\hat{n}_1^* &= \hat{\ell}_f = (\cos\delta_f\cos\alpha_f)\hat{n}_1 + (\cos\delta_f\sin\alpha_f)\hat{n}_2 + (\sin\delta_f)\hat{n}_3 \\
\hat{\ell}_o &= (\cos\delta_o\cos\delta_o)\hat{n}_1 + (\cos\delta_o\sin\alpha_o)\hat{n}_2 + (\sin\delta_o)\hat{n}_3 \\
\hat{n}_3^* &= \hat{\ell}_f \times \hat{\ell}_o/|\hat{\ell}_f \times \hat{\ell}_o| \\
\hat{n}_2^* &= \hat{n}_3^* \times \hat{n}_1^*
\end{aligned} \tag{8.26}$$

Equations 8.26 can be collected in matrix form as

$$\{\hat{n}^*\} = [C]\{\hat{n}\} \tag{8.27}$$

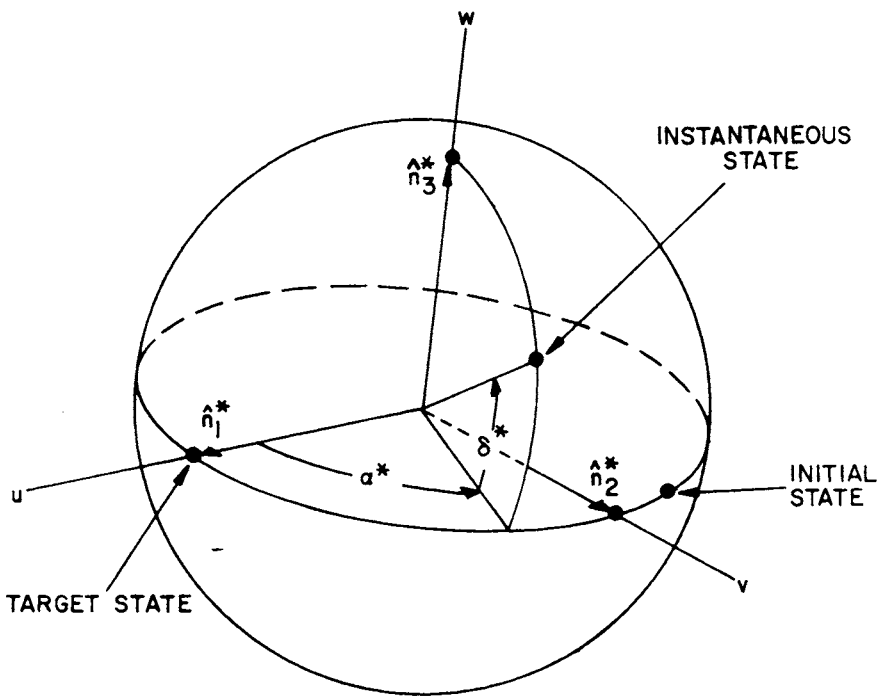

Figure 8.2 Initial State/Target State Inertial Reference System

TABLE 8.1

TYPICAL NOVA PARAMETERS

t_o = year 1980, day 320, hour 12, min 0 (GMT)

M = 69,600 pole-cm = 69.600 amp-m^2

$\dot{\phi}$ = 5 rpm

I_3 = 34 kg-m^2

a = orbit semimajor axis = 1.102818 Earth radii

e = eccentricity = 0.029192

i = inclination = 89.290 deg

ω = arg. of perigee = 24.870 deg

Ω = arg. of ascending node = 366.602 deg

di/dt = 0

$d\omega/dt$ = -3.536 deg/day

$d\Omega/dt$ = -0.0876 deg/day

where [C] is the resulting constant direction cosine matrix. The optimal control formulation of Section 8.2.3 remains valid for this special inertial frame; it is necessary to (everywhere above) replace [R] of Eq. 8.16 by

$$[R^*] = [R][C^T] \tag{8.28}$$

In the event of near 180 deg maneuvers, we take (in lieu of the last of Eq. 8.26)

$$\hat{n}_3^* = \hat{\ell}_f \times \hat{n}_3$$

To avoid ambiguity, we use (α^*,δ^*) to denote the angles analogous to (α,δ) defined with respect to $\{\hat{n}^*\}$. Note the desired consequence that $[\alpha^*(t_o), \delta^*(t_o)]$ and $[\alpha^*(t_f), \delta^*(t_f)]$ locate points on the "equator" of the $\{\hat{n}^*\}$ system, and the final state $[\alpha^*(t_f), \delta^*(t_f)]$ lies at either the origin (0,0) or $(2\pi,0)$; these properties simplify and universalize methods for interactively solving the TPBVP.

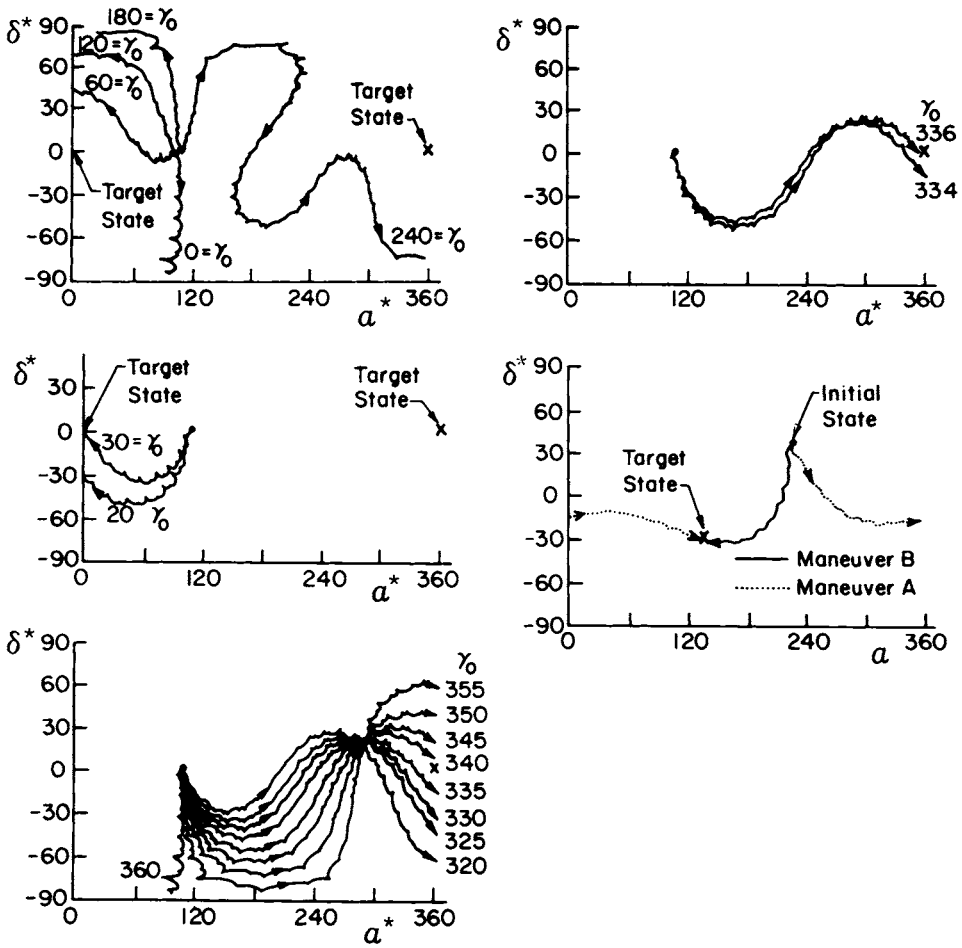

Figures 8.3 - 8.7 Interactive Extremal Field Map Iterations to Determine Minimum Time Magnetic Attitude Maneuvers

Table 8.2

Optimal Maneuver A

Command no.	Day	Hour	Minute	p(t)	$\alpha(t)$	$\delta(t)$
1	320	12	0	-1	45.2	35.1
2	320	12	17	1	39.7	29.7
3	320	12	45	-1	44.2	22.4
4	320	13	9	1	40.8	17.9
5	320	13	32	-1	42.9	10.5
6	320	13	57	1	36.5	4.1
7	320	14	23	-1	37.6	-2.8
8	320	14	49	1	31.0	-6.1
9	320	15	11	-1	30.8	-12.4
10	320	15	37	1	21.8	-17.2
11	320	16	1	-1	20.1	-22.6
12	320	16	28	1	9.8	-23.7
13	320	16	50	-1	7.0	-27.9
14	320	17	17	1	-4.7	-29.9
15	320	17	39	-1	-9.1	-32.7
16	320	18	8	1	-21.5	-31.0
17	320	18	30	-1	-26.0	-32.8
18	320	18	57	1	-38.3	-32.0
19	320	19	12	0	-42.7	-31.4

To illustrate the determination of optimal maneuvers using the above developments, we adopt the NOVA vehicle and orbit parameters in Table 8.1. The objective is to find the sequence of switching times to maneuver from the initial state (α_0 = 45.2°, δ_0 = 35.1°) to the desired final state (α_f = -45.0° δ_f = -30.0°).

Figure 8.3 displays an extremal field of trajectories (relative to $\{n^*\}$ generated by sweeping γ_0 from 0° to 360° at an increment of 60°); this rather large step was taken to allow an interactive graphics user to immediately note that the trajectories passing near the origin appear to be contained in the interval (0° < γ_0 < 60°) and that trajectories to the point X (360°,0) appear

Table 8.3

Optimal Maneuver B

Command no.	Day	Hour	Minute	p(t)	α(t)	δ(t)
1	320	12	0	-1	45.2	35.1
2	320	12	9	1	44.3	31.0
3	320	12	39	-1	54.4	25.1
4	320	13	1	1	56.4	21.2
5	320	13	27	-1	63.7	15.1
6	320	13	46	1	65.6	10.1
7	320	14	15	-1	75.3	4.9
8	320	14	37	1	77.2	0.8
9	320	15	4	-1	85.7	-3.2
10	320	15	23	1	88.2	-7.1
11	320	15	51	-1	99.0	-10.1
12	320	16	12	1	101.7	-14.2
13	320	16	40	-1	112.2	-14.7
14	320	16	59	1	115.2	-17.0
15	320	17	27	-1	127.3	-17.5
16	320	17	48	1	131.3	-20.2
17	320	18	17	-1	142.3	-17.6
18	320	18	36	1	146.1	-19.0
19	320	19	3	-1	157.6	-17.5
20	320	19	24	1	162.3	-18.1
21	320	19	52	-1	172.8	-15.2
22	320	20	12	1	176.6	-15.8
23	320	20	40	-1	-172.2	-13.5
24	320	21	0	1	-167.8	-12.7
25	320	21	28	-1	-157.5	-12.0
26	320	21	48	1	-153.8	-12.0
27	320	22	17	-1	-142.6	-10.9
28	320	22	36	1	-138.4	-10.6
29	320	23	5	-1	-128.0	-12.1
30	320	23	24	1	-124.3	-11.7
31	320	23	54	-1	-113.0	-12.9
32	321	0	13	1	-109.2	-14.0
33	321	0	42	-1	-98.5	-16.1
34	321	1	1	1	-95.0	-16.8
35	321	1	30	-1	-83.5	-19.9
36	321	1	50	1	-79.7	-21.9
37	321	2	20	-1	-68.2	-22.9
38	321	2	38	1	-64.7	-25.1
39	321	3	7	-1	-52.2	-28.0
40	321	3	27	1	-48.0	-29.6
41	321	3	30	0	-47.8	-29.8

to be contained in the interval ($180° < \gamma_0 < 360°$). Subsequent exploration (Fig. 8.4) for the optimal trajectory ("Extremal A") to the origin reveals $\gamma_0 \cong 30°$ generates the desired extermal. Extermal A required a maneuver time of 7.20 h and 19 polarity switches (Table 8.2) to complete the maneuver. The results of Table 8.2 were generated by integrating Eq. 8.4b and reflect about 2° accumulated errors from the approximations implicit in Eqs. 8.6.

The search for the second solution in the interval ($180° < \gamma_0 < 360°$) is more laborious, but two intermediate trials led to the family of trajectories displayed in Fig. 8.5; it is evident that the solution lies in the interval ($335° < \gamma_0 < 340°$). One subsequent iteration (Fig. 8.6) reveals that $\gamma_0 = 336°$ generates Extremal B; this solution requires a maneuver time of 15.50 h and 41 polarity switches (Table 8.3). The longer maneuver time of 15.5 h does not result in a large error accumulation ($\approx$ 3 deg). It is anticipated, in actual implementations, that a restart will be done after typically 10 h of maneuver time to reduce the accumulation of these errors to < 2°. It is not surprising that the smaller angle maneuver (Extremal A) was found to be preferable (vis-a-vis maneuver time) than maneuver B. Intuition will prove less reliable for maneuvers near 180°, mainly due to Earth rotation and orbital eccentricity effects, but also due to asymmetries in the geomagnetic field.

The (α,δ) history of maneuvers A and B are displayed in Fig. 8.7. The fine structure precession cusps of Figs. 8.4 and 8.6 are not in evidence since the curves of Fig. 8.7 are simply straight-line connections of the states at polarity switch times.

The entire sequence of calculations and displays (underlying in Figs. 8.3-8.7 and Tables 8.1-8.3) were generated in less than 15 min of real time. It has been found much more attractive to display successive trajectory families on an interactive CRT, rather than constructing an elaborate search logic to

automate selection of the optimal solution of the TPBVP. Numerical searches (for the point of closest approach along each trial trajectory) are difficult to implement reliably due to the many local minima associated with polarity switch cusps. However, an engineer can glance at a CRT display of the field of optimal trajectories and make the selection reliably in an interactive fashion.

The possibility of singular sub-arcs (along which the switch function, Eq. 8.22, identically vanishes) is a mathematical possibility; the existence of these cases is not dealt with formally here, although our numerical results suggest that they do not exist for practical values of the Earth's magnetic field constants and near-earth orbits. The maneuvers are not generally unique, in the sense that at least two maneuvers between the same terminal points generally exist. Except within ± 10° of the 180° transfer case, we can usually discard the solution requiring greater than 180° slewing since it will almost always require a longer maneuver time. Also, maneuvers with periods near integer multiples of twelve hours often exhibit multiple extrema due to near-periodic effects associated with earth rotation and near-symmetry of the magnetic field. This latter truth is evident in Figure 8.5. All of the trajectories shown pass near (300°, 20°) about twelve hours into the maneuver. Again, the existence of such local extrema is evident by interactively studying the extremal field of trajectories.

8.2.4 Concluding Remarks on Minimum Time Magnetic Maneuvers

During May 1981, the NOVA-1 spacecraft was launched and the above approach was used to carry out several large angle, minimum time maneuvers. These maneuvers were required to (i) adjust the orbit radius and inclination (the single rocket motor is aligned with the spin axis and must be pointed in the desired inertial direction before each orbit adjust), (ii) adjust the angular phase in the orbit and finally (iii) to obtain the final radial pointing prior

to boom extension and gravity gradient capture. All maneuvers were commanded in an "open loop" fashion with numerous switch commands for several hours of magnetic maneuvers being calculated (in ground-based computers) and uploaded to the on-board computer which actually generates the magnet current polarity control commands. Several manevuers exceeding six hours and 45° reorientation were performed with residual errors of less than two degrees. Final "trim" maneuvers were then used to null these errors. It proved necessary to modify the above developments slightly to accomodate power consumption constraints (see Ref. 19 for details).

The above developments and the successful application to NOVA represents an elegant "real world" example in which optimal control theory leads directly to an easily implemented and most useful control for a nonlinear system. The successful implementation of the NOVA spacecraft magnetic maneuvers is a gratifying demonstration of the practical utility of optimal control theory.

8.3 OPTIMAL MOMENTUM TRANSFER MANEUVERS

8.3.1 Background

In Section 4.4, we considered the manevuers of a rigid spacecraft B containing a single reaction wheel W (Fig. 4.7). In the initial state, the wheel is locked and the rigid vehicle is spinning uniformly about its largest inertia axis ($\hat{b}_3$) (colinear with the inertially constant angular momentum vector). The objective is to align, as nearly as possible, the $\hat{b}_2$ axis with the constant angular momentum vector, while bringing the body B to rest. For a spacecraft, this usually corresponds to transferring from a spin stabilized mode to a three-axis control mode. Physically, the objective is to transfer all of the system energy and momentum into the wheel by using a judicious motor torque history. In Section 4.4.2 we considered perhaps the simplest torque policy, namely the nearly constant torque required to cause a constant

acceleration of the wheel relative to the body. An example ensuing maneuver is shown in Fig. 4.8.

For contrast with the *heuristic torque maneuver* of Section 4.4.2, as shown in Figs. 4.8, 4.9, we consider applying here optimality criteria to find an optimal maneuver for comparison.

8.3.2 Formulation of the Necessary Conditions

It is evident from Sections 4.4.1, 4.4.2 that no sequential combination of constant and zero torque will achieve the maneuver exactly (in finite time). Thus, we anticipate that the desired final state $\omega_i(t_f) = 0$, $i = 1,2,3$, is not exactly reachable. This motivates choosing the performance index

$$J = \frac{w}{2}\left[\omega_1^2(t_f) + \omega_2^2(t_f) + \omega_3^2(t_f)\right] + \frac{1}{2}\int_{t_o}^{t_f} u^2(t)dt \qquad (8.29)$$

where w is a positive weight which allows relative emphasis to be placed upon small final angular velocity errors versus small control torque history. In the example below, we take w = 1.

From Eqs. 4.89 through 4.92, the spacecraft and wheel state dynamics are governed by the four nonlinear first order equations

$$\dot{\omega}_1 = -I_1\,\omega_2\omega_3 + \omega_3\,h/I_1 \equiv f_1(\omega_1,\omega_2,\omega_3,h,u) \qquad (8.30a)$$

$$\dot{\omega}_2 = -I_2\,\omega_1\omega_3 - u/I_2^* \equiv f_2(\omega_1,\omega_2,\omega_3,h,u) \qquad (8.30b)$$

$$\dot{\omega}_3 = -I_3\,\omega_1\omega_2 - \omega_1 h/I_3 \equiv f_3(\omega_1,\omega_2,\omega_3,h,u) \qquad (8.30c)$$

$$\dot{h} = -I_4\,\omega_1\omega_3 + u(I_2/I_2^*) \equiv f_4(\omega_1,\omega_2,\omega_3,h,u) \qquad (8.30d)$$

where $h = J_2\,\Omega_2$ is the wheel relative momentum

$$I_1, I_2, I_3, I_4 \equiv \left(\frac{I_3-I_2}{I_1}\right),\ \left(\frac{I_1-I_3}{I_2^*}\right),\ \left(\frac{I_2-I_1}{I_3}\right),\ J_2\left(\frac{I_3-I_1}{I_2^*}\right)$$

(I_1^*, I_2^*, I_3^*) the principal inertias of B

$(I_i = I_i^* + J_i,\ i = 1,2,3)$, the inertias of the composite body B + W.

and u is the motor torque we wish to optimize.

We seek to minimize the performance functional of Eq. 8.29 subject to satisfying Eq. 8.30 with the specified initial state

$$\{\omega_1(t_o) = 0 \quad , \quad \omega_2(t_o) = 0 \quad , \quad \omega_2(t_o) = \omega_{30} \quad , \quad h(t_o) = 0\} \tag{8.31}$$

The final state is not fully specified, but we have the momentum transfer condition

$$h(t_f) = |\mathbf{H}| = H = I_3\omega_{30} \tag{8.32}$$

and we choose to leave the remaining final state variables $\{\omega_i(t_f) \quad i = 1,2,3\}$ *free*. Implicitly, we are relying upon the first term of the performance functional to make the $\omega_i(t_f)$ small. Thus, we anticipate the necessity of using *transversality* conditions in lieu of prescribing values for the $\omega_i(t_f)$.

We define the Hamiltonian Functional

$$H = \frac{1}{2} u^2 + \sum_{i=1}^{4} \lambda_i f_i \tag{8.33}$$

and apply Pontryagin's principle (Eqs. 6.36 through 6.40) to find the remaining necessary conditions for optimality. The co-state variables satisfy the adjoint differential equations

$$\dot{\lambda}_i = -\frac{\partial H}{\partial \omega_i} = -\sum_{j=1}^{4} \frac{\partial f_j}{\partial \omega_i} \lambda_j \quad , \quad i = 1,2,3 \text{ and } \dot{\lambda}_4 = -\frac{\partial H}{\partial h} = -\sum_{j=1}^{4} \frac{\partial f_i}{\partial h} \lambda_j$$

or, explicitly

$$\begin{Bmatrix} \dot{\lambda}_1 \\ \dot{\lambda}_2 \\ \dot{\lambda}_3 \\ \dot{\lambda}_4 \end{Bmatrix} = \begin{bmatrix} 0 & I_2\omega_3 & I_3\omega_2 & I_4\omega_3 \\ I_1\omega_3 & 0 & I_3\omega_1 & 0 \\ I_1\omega_1 & I_2\omega_1 & 0 & I_4\omega_1 \\ -\omega_3/I_1 & 0 & \omega_1/I_3 & 0 \end{bmatrix} \begin{Bmatrix} \lambda_1 \\ \lambda_2 \\ \lambda_3 \\ \lambda_4 \end{Bmatrix} \tag{8.34}$$

and the optimal control (assumed continuous, smooth, and unbounded) is determined from $\frac{\partial H}{\partial u} = 0$ as

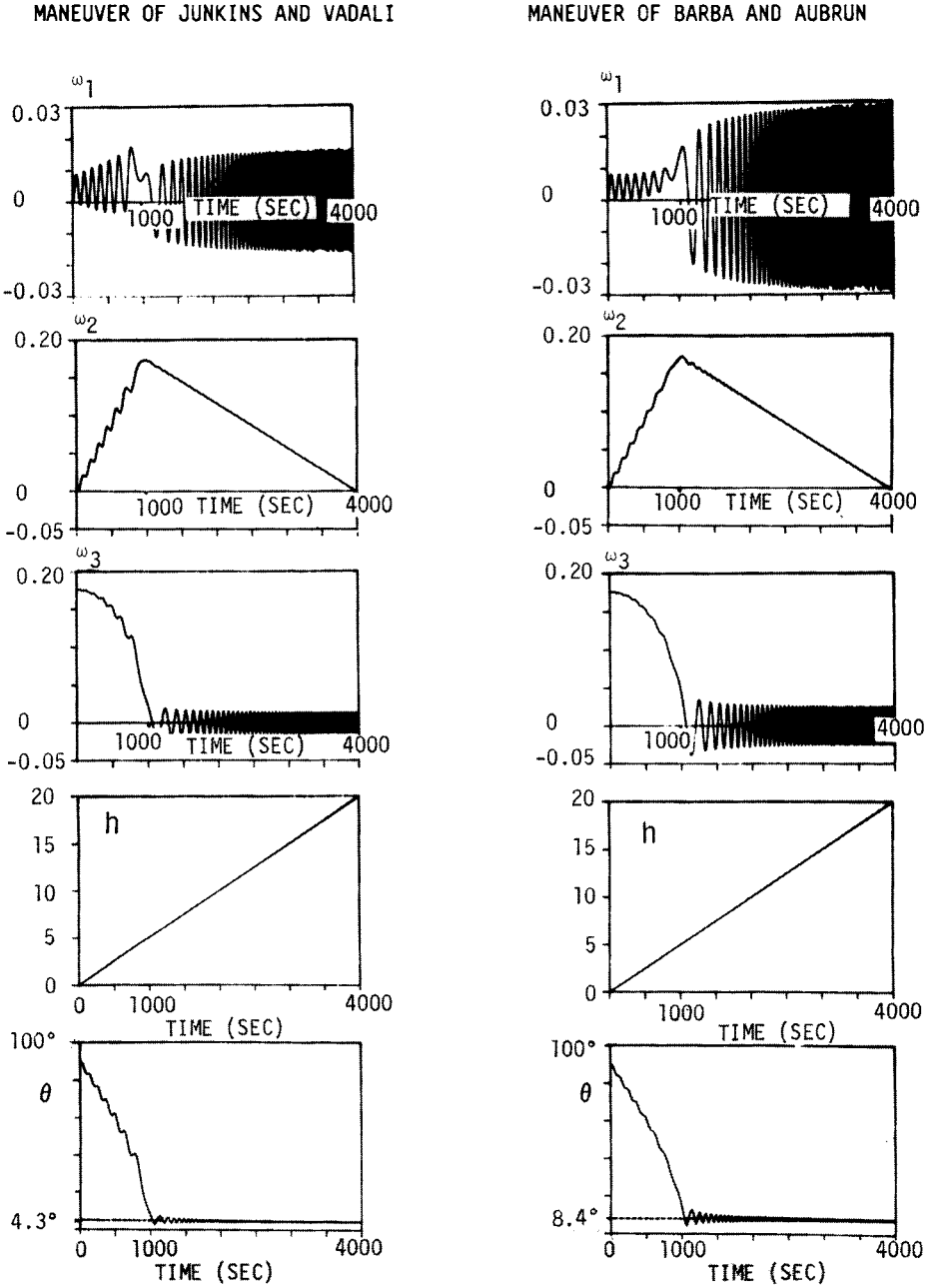

Figure 8.8 A Comparison of Two Flat Spin Recovery Maneuvers

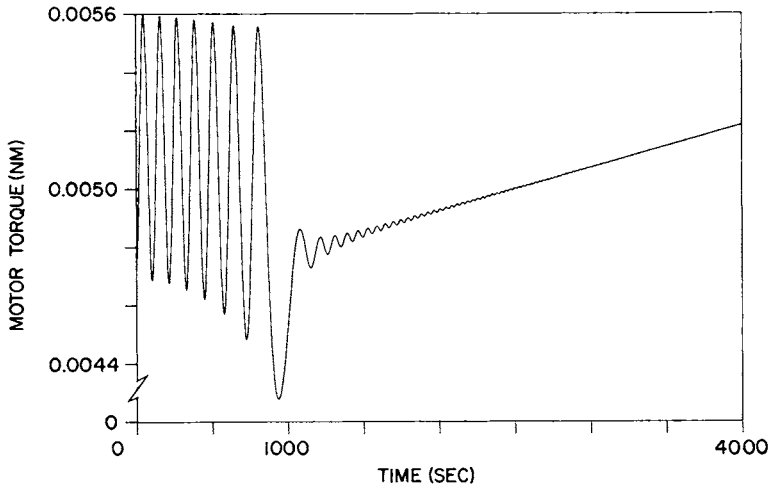

Figure 8.9 Optimal (Junkins and Vadali) Motor Torque History for a Flat Spin Recovery

$$u = -\sum_{i=1}^{4} \frac{\partial f_i}{\partial u} \lambda_i = \left(\frac{1}{I_2^*}\right)\lambda_2 - \left(\frac{I_2}{I_2^*}\right)\lambda_4 \tag{8.35}$$

The $\omega_i(t_f)$ being free, dictate from Eq. 6.40 the final transversality conditions

$$\lambda_i(t_f) = w\,\omega_i(t_f) \quad , \quad i = 1,2,3 \tag{8.36}$$

Thus, we have eight differential equations (Eqs. 8.30, 8.34, using Eq. 8.35) and eight boundary conditions (Eqs. 8.31, 8.32, and 8.36). Notice, we have the four initial conditions of Eqs. 8.31, and the four final conditions of Eqs. 8.32, 8.36; thus we have a nonlinear TPBVP, as expected. However, we have a further complication, since the $\omega_i(t_f)$ are "free" and unknown, we cannot determine from Eq. 8.36 specific numerical values for the $\lambda_i(t_f)$. Rather, Eq. 8.36 represents a condition on $\lambda_i(t_f)$ and $\omega_i(t_f)$ which implicitly depends upon the known $\omega_i(t_0)$, $h(t_0)$ and the *unknown* $\lambda_i(t_0)$. Since we have an a priori, sub-optimal solution of Section 4.4.2, we are motivated to seek a solution near

this one as a starting iterative. Note, for w = 1 and if the optimum $\omega_i(t_f)$ are small, (as desired) we see from Eq. 8.36 that $\lambda_i(t_f)$, i = 1,2,3 are also small. It is clear from Eq. 8.34 that $\lambda_i(t_f) \equiv 0$, i = 1,2,3,4 results in $\lambda_i(t) \equiv 0$ for all time and, furthermore, suggests that small $\lambda_i(t_f)$ will result in small $\lambda_i(t)$, at least for $|t - t_f|$ small. Thus we are motivated to try the initial (k = 0) trial values

$$\lambda_i(t_o) = 0 \quad , \quad i = 1,2,3$$

for the first three co-state initial values. For $\lambda_4(t_o)$, we can make use of the fact that the sub-optimal constant torque level is 0.05 N.m. (from Section 4.4.1), so we find a consistent initial (k = 0) trial value for $\lambda_4(t_o)$ from Eq. 8.35 as

$$\lambda_4(t_o) = - \frac{0.005}{(I_2/I_2^*)}.$$

Without discussing details of the numerical solution process (the interested reader is referred to Reference 15), we present the optimal maneuver determined by the Method of Particular Solutions (see Chapter 7). The optimal maneuver [the solutions of Eqs. 8.30, 8.31, 8.32, 8.34, 8.35, 8.36 which minimizes Eq. 8.29, over all continuous, differentiable u(t)] is shown in Figures 8.8 and 8.9. Comparing this optimal maneuver with Barba and Aubrun's maneuver of Figure 4.8 (determined by taking $\dot{h}$ = 0.005 = constant), we see that the two maneuvers are indeed qualitatively quite similar. Note that h(t) looks graphically almost identical for the two maneuvers. However, as is evident in Figure 8.9, the optimal $\dot{h}(t)$ and the optimal torque are indeed ±10% variable about the nominal constant value of 0.005 NM (of the Barba and Auburn maneuver). These ±10% optimal torque variations have the following desirable impacts upon the maneuver:

(i) The peak amplitude of the final ω_1, ω_3 oscillations are reduced by factor of 2.

(ii) The final nutation angle ($\hat{b}_2$ coning about H) is reduced substantially from 8.4^0 to 4.3^0 (see the graphs in figure 8.8).

However, the optimal torque history oscillates ±10% about 0.005 mm in a relatively "busy" fashion during the first 1000 seconds and would therefore be more difficult to implement. Also, simulations indicate that this optimum control is more sensitive to model parameter variations (due to uncertainty in the actual system's model parameters and unmodeled disturbance effects). In this particular case, having computed the optimal maneuver simply serves as excellent justification for the much easier to implement heuristic maneuver of Figure 4.8. For several reaction wheels, and including a general prescription of initial and final orientation and angular velocity states, however, such simple heuristic controls become extraordinarily difficult to specify a priori. We could view the availability of optimal maneuvers as serving two functions: (i) providing a standard for evaluating performance loss associated with sub-optimal maneuvers, and (ii) providing the optimal control history to suggest simple forms for easy-to-implement sub-optimal controls. In some practical problems, the optimal maneuvers are as easy to implement as a sub-optimal maneuver, as was the case for the NOVA minimum time maneuvers (Section 8.2). Several subsequent examples of this chapter further illustrate this point.

8.4 THREE WHEEL MOMENTUM TRANSFER MANEUVERS

8.4.1 Equations of Motion

To generalize the above manevuers, we consider the three identical reaction wheel configuration shown in Figure 8.10. The equations of motion follow from Section 4.4.3 or can be specifically developed from first principles as follows. The system angular momentum is

$$H = H_{SPACECRAFT} + H_{WHEELS}$$

or

$$H = I_1^*\omega_1\hat{b}_1 + I_2^*\omega_2\hat{b}_2 + I_3^*\omega_3\hat{b}_3$$
$$+ [J_a(\omega_1 + \Omega_1)\hat{b}_1 + J_t\omega_2\hat{b}_2 + J_t\omega_3\hat{b}_3]$$
$$+ [J_t\omega_1\hat{b}_1 + J_a(\omega_2 + \Omega_2)\hat{b}_2 + J_t\omega_3\hat{b}_3]$$
$$+ [J_t\omega_1\hat{b}_1 + J_t\omega_2\hat{b}_2 + J_a(\omega_3 + \Omega_3)\hat{b}_3]$$

or

$$H = (I_1^* + J_a + 2J_t)\omega_1\hat{b}_1 + (I_2^* + J_a + 2J_t)\omega_2\hat{b}_2 + (I_3^* + J_a + 2I_t)\omega_3\hat{b}_3$$
$$+ J_a\Omega_1\hat{b}_1 + J_a\Omega_2\hat{b}2 + J_a\Omega_3\hat{b}_3 \qquad (8.36)$$

where

$(\omega_1,\omega_2,\omega_3)$ are spacecraft angular velocities

$(\Omega_1,\Omega_2,\Omega_3)$ are relative wheel speeds

(I_1^*,I_2^*,I_3^*) are spacecraft inertias

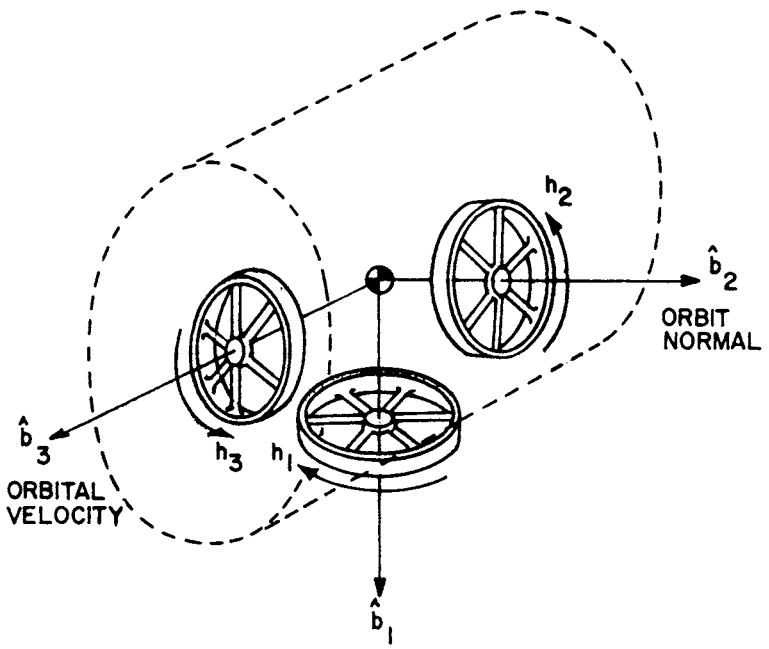

Figure 8.10 Asymmetric Rigid Spacecraft Containing Three Orthogonal Reaction Wheels

J_a is the axial inertia of each wheel

J_t is the transverse inertia of each wheel.

We define

$I_i = I_i^* + J_a + 2I_t$, composite body (spacecraft plus wheels) inertias

$h_i = J_a\Omega_i$, relative wheel momenta,

then Eq. 8.36 can be written as

$$\mathbf{H} = (I_1\omega_1 + h_1)\hat{\mathbf{b}}_1 + (I_2\omega_2 + h_2)\hat{\mathbf{b}}_2 + (I_3\omega_3 + h_3)\hat{\mathbf{b}}_3$$

The spacecraft equations of motion then follow from the Euler equation of rotational motion:

$$\dot{\mathbf{H}} = \mathbf{0} = [\sum_{i=1}^{3} (I_i\dot{\omega}_i + \dot{h}_i)\hat{\mathbf{b}}_i] + [\sum_{j=1}^{3} \omega_i\hat{\mathbf{b}}_i] \times [\sum_{i=1}^{3} (I_i\omega_i + h_i)\hat{\mathbf{b}}_i] \tag{8.37}$$

as

$$\begin{aligned} I_1\dot{\omega}_1 + \dot{h}_1 &= (I_2 - I_3)\omega_2\omega_3 - h_3\omega_2 + h_2\omega_3 \\ I_2\dot{\omega}_2 + \dot{h}_2 &= (I_3 - I_1)\omega_3\omega_1 - h_1\omega_3 + h_3\omega_1 \\ I_3\dot{\omega}_3 + \dot{h}_3 &= (I_1 - I_2)\omega_1\omega_2 - h_2\omega_1 + h_1\omega_2 \end{aligned} \tag{8.38}$$

The wheel equations of motion follow from *motor torque* = $\frac{d}{dt}$ *(axial angular momentum)* as

$$u_i = J_a\dot{\omega}_i + \dot{h}_i \quad , \quad i = 1,2,3 \tag{8.39}$$

Equations 8.38, 8.39 can be solved for $(\dot{\omega}_i, \dot{h}_i)$ to obtain

$$\begin{aligned} (I_1 - J_a)\dot{\omega}_1 &= (I_2 - I_3)\omega_2\omega_3 - h_3\omega_2 + h_2\omega_3 - u_1 \\ (I_2 - J_a)\dot{\omega}_2 &= (I_3 - I_1)\omega_3\omega_1 - h_1\omega_3 + h_3\omega_1 - u_2 \\ (I_3 - J_a)\dot{\omega}_3 &= (I_1 - I_2)\omega_1\omega_2 - h_2\omega_1 + h_1\omega_2 - u_3 \\ \dot{h}_i &= -J_a\dot{\omega}_i + u_i \quad , \quad i = 1,2,3 \end{aligned} \tag{8.40}$$

Equations 8.40 together with the Euler parameter kinematic equation

$$\begin{Bmatrix} \dot{\beta}_0 \\ \dot{\beta}_1 \\ \dot{\beta}_2 \\ \dot{\beta}_3 \end{Bmatrix} = \frac{1}{2} \begin{bmatrix} \beta_0 & -\beta_1 & -\beta_2 & -\beta_3 \\ \beta_1 & \beta_0 & -\beta_3 & \beta_2 \\ \beta_2 & \beta_3 & \beta_0 & -\beta_1 \\ \beta_3 & -\beta_2 & \beta_1 & \beta_0 \end{bmatrix} \begin{Bmatrix} 0 \\ \omega_1 \\ \omega_2 \\ \omega_3 \end{Bmatrix} \tag{8.41}$$

constitute a tenth-order system of nonlinear equations of the functional form

$$\dot{x}_i = f_i(x_1, \ldots, x_{10}, u_1, u_2, u_3) \quad , \quad i = 1,2,,\ldots,10$$

or

$$\dot{\mathbf{x}} = \mathbf{f}(\mathbf{x}, \mathbf{u}) \tag{8.42}$$

with

$$\mathbf{x} = [\omega_1 \ \omega_2 \ \omega_3 \ h_1 \ h_2 \ h_3 \ \beta_0 \ \beta_1 \ \beta_2 \ \beta_3]^T.$$

The Euler parameters satisfy the constraint $\beta^T\beta = 1$ and, since external torques are zero, $\dot{H} = 0$ or H = constant. These two constraints are implicit, but certain advantages are realized by making explicit use of H = constant. The β's orient the body axes $\{\hat{\mathbf{b}}\}$ with respect to the arbitrary inertial frame $\{\hat{\mathbf{n}}\}$ in the sense of the orthogonal projection:

$$\{\hat{\mathbf{b}}\} = [C(\beta)]\{\hat{\mathbf{n}}\} \tag{8.43}$$

where (Chapter 2)

$$[C(\beta)] = \begin{bmatrix} \beta_0^2+\beta_1^2-\beta_2^2-\beta_3^2 & 2(\beta_1\beta_2+\beta_0\beta_3) & 2(\beta_1\beta_3-\beta_0\beta_2) \\ 2(\beta_1\beta_2-\beta_0\beta_3) & \beta_0^2-\beta_1^2+\beta_2^2-\beta_3^2 & 2(\beta_2\beta_3+\beta_0\beta_1) \\ 2(\beta_1\beta_3+\beta_0\beta_2) & 2(\beta_2\beta_3-\beta_0\beta_1) & \beta_0^2-\beta_1^2-\beta_2^2+\beta_3^2 \end{bmatrix} \tag{8.44}$$

We introduce a special inertial frame $\{\hat{\mathbf{h}}\}$ chosen with $\hat{\mathbf{h}}_2$ aligned with $\mathbf{H}$, the orientation of $\hat{\mathbf{h}}_1$ and $\hat{\mathbf{h}}_3$ can be chosen by any convenient rule, so long as perpendicular to each other and $\hat{\mathbf{h}}_2$. Thus we have another set of Euler parameters $\delta = (\delta_0, \delta_1, \delta_2, \delta_3)^T$ orienting $\{\hat{\mathbf{b}}\}$ relative to $\{\hat{\mathbf{h}}\}$ in the sense

$$\{\hat{\mathbf{b}}\} = [C(\delta)]\{\hat{\mathbf{h}}\} \tag{8.45}$$

Of course, the orientation of $\{\hat{\mathbf{h}}\}$ relative to the inertial frame $\{\hat{\mathbf{n}}\}$ is constant and can also be parameterized in terms of a constant set of Euler

parameters α as

$$\{\hat{h}\} = [C(\alpha)]\{\hat{n}\} \tag{8.46a}$$

These constant Euler parameters can be calculated (see Ref. 15) as

$$\alpha_o = \frac{H + H_{n_2}}{2H} \quad , \quad \alpha_2 = 0$$

$$\alpha_1 = -H_{n_3}\left[\frac{H - H_{n_2}}{2H(H_{n_1}^2 + H_{n_2}^2)}\right]^{1/2} \quad , \quad \alpha_3 = H_{n_1}\left[\frac{H - H_{n_2}}{2H(H_{n_1}^2 + H_{n_3}^2)}\right]^{1/2} \tag{8.46b}$$

where the H_{n_i} are the constant $\hat{n}_i$ components of the angular momentum vector. The three sets of Euler parameters are related (Chapter 2) by the successive rotation result

$$\begin{Bmatrix} \delta_o \\ \delta_1 \\ \delta_2 \\ \delta_3 \end{Bmatrix} = \begin{bmatrix} \beta_o & -\beta_1 & -\beta_2 & -\beta_3 \\ \beta_1 & \beta_o & \beta_3 & -\beta_2 \\ \beta_2 & -\beta_3 & \beta_o & \beta_1 \\ \beta_3 & \beta_2 & -\beta_1 & \beta_o \end{bmatrix} \begin{Bmatrix} \alpha_o \\ \alpha_1 \\ \alpha_2 \\ \alpha_3 \end{Bmatrix} \tag{8.47}$$

which, given any two sets of Euler parameters, can be solved for the third. The body components H_{b_i} of the angular momentum vector H can be directly calculated in terms of H, δ as

$$\begin{Bmatrix} H_{b_1} \\ H_{b_2} \\ H_{b_3} \end{Bmatrix} = [C(\delta)] \begin{Bmatrix} 0 \\ H \\ 0 \end{Bmatrix} = \begin{Bmatrix} 2(\delta_1\delta_2 + \delta_o\delta_3)H \\ (\delta_o^2 - \delta_1^2 + \delta_2^2 - \delta_3^2)H \\ 2(\delta_2\delta_3 - \delta_o\delta_1)H \end{Bmatrix} \tag{8.48}$$

Since $H_{b_i} = I_i\omega_i + h_i$, it is evident that the wheel momenta can be explicitely eliminated in terms of the ω_i, δ_i and the constant H as

$$\begin{Bmatrix} h_1 \\ h_2 \\ h_3 \end{Bmatrix} = \begin{Bmatrix} 2H(\delta_1\delta_2 + \delta_o\delta_3) - I_1\omega_1 \\ H(\delta_o^2 - \delta_1^2 + \delta_2^2 - \delta_3^2) - I_2\omega_2 \\ 2H(\delta_2\delta_3 - \delta_o\delta_1) - I_3\omega_3 \end{Bmatrix} \tag{8.49}$$

Thus, using Eq. 8.49 in Eqs. 8.40, we can reduce the order of the system from

ten to seven. The independent elements of the state vector are then

$$x = (\omega_1,\omega_2,\omega_3,\delta_0,\delta_1,\delta_2,\delta_3)^T \tag{8.50}$$

In lieu of Eq. 8.41, we have the same equation with $\beta_i \to \delta_i$.

8.4.2 Optimal Control Formulation

The first issue is the selection of a performance index. We consider three indices based upon quadratic penalties on the control magnitude and derivatives thereof:

$$J_1 = \frac{1}{2}\int_0^T \left(\sum_{i=1}^3 u_i^2(t)dt\right) = \int_0^T f_1\, dt \tag{8.51}$$

$$J_2 = \frac{1}{2}\int_0^T \left(\sum_{i=1}^3 \dot{u}_i^2(t)\right)dt = \int_0^T f_2\, dt \quad , \quad \dot{u}_i = \frac{d}{dt}u_i \tag{8.52}$$

$$J_3 = \frac{1}{2}\int_0^T \left(\sum_{i=1}^3 \ddot{u}_i^2(t)\right)dt = \int_0^T f_3\, dt \quad , \quad \ddot{u}_i = \frac{d^2}{dt^2}u_i \tag{8.53}$$

In addition, for each optimal maneuver, we determine a positive measure of electrical energy expenditure, by computing the following integral (E):

$$E = \int_0^T \sum_{i=1}^3 |u_i(t)\Omega_i(t)|dt \tag{8.54}$$

as a "side calculation".

In preparation for formulating the Pontryagin necessary conditions we introduce the Hamiltonian (for J_1)

$$H_1 = \frac{1}{2}\sum_{i=1}^3 u_i^2 + \sum_{i=0}^3 \gamma_i\dot{\delta}_i + \sum_{i=1}^3 \lambda_i\dot{\omega}_i \tag{8.55}$$

where analogous Hamiltonians can be defined for indices J_2, J_3. The γ_i's and λ_i's are the co-state (Lagrange Multiplier) variables. The Hamiltonian of Eq. 8.55 is explicitly

$$H_1 = \frac{1}{2}(u_1^2 + u_2^2 + u_3^2) + \gamma_0(-\omega_1\delta_1 - \omega_2\delta_2 - \omega_3\delta_3)$$

$$+ \gamma_1(\omega_1\delta_0 - \omega_2\delta_3 + \omega_3\delta_2) + \gamma_2(\omega_1\delta_3 + \omega_2\delta_0 - \omega_3\delta_1)$$

$$+ \gamma_3(-\omega_1\delta_2 + \omega_2\delta_1 + \omega_3\delta_o) \tag{8.56}$$

$$+ \lambda_1(-H_{b_3}\omega_2 + H_{b_2}\omega_3 - u_1)/(I_1 - J_a)$$

$$+ \lambda_2(-H_{b_1}\omega_3 + H_{b_3}\omega_1 - u_2)/(I_2 - J_a)$$

$$+ \lambda_3(-H_{b2}\omega_1 + H_{b1}\omega_2 - u_3)/(I_3 - J_a)$$

Since $u_i(t)$ are assumed smooth and unconstrained on (0,T) the optimally criteria for an extremum of H_1 are:

$$\frac{\partial H_1}{\partial u_i} = 0 = u_i - \lambda_i/(I_i - J_a) \quad , \quad i = 1,2,3 \tag{8.57}$$

This extremum is a minimum, since

$$\frac{\partial^2 H_1}{\partial u_i^2} = 1 > 0 \quad , \quad i = 1,2,3 \tag{8.58}$$

The optimal torque histories are now expressed in terms of the optimal co-states by rearranging Eq. 8.57 as

$$u_i(t) = \lambda_i(t)/(I_i - J_a) \quad , \quad i = 1,2,3 \tag{8.59}$$

The state and co-state equations obtained by the application of Pontryagin's principle (Chapter 6) (u_i is eliminated in the terms of the respective λ_i from Eqs. 8.40) are summarized below:

State Equations

$$\begin{aligned}
\dot{\delta}_o &= (-\omega_1\delta_1 - \omega_2\delta_2 - \omega_3\delta_3)/2 \\
\dot{\delta}_1 &= (\omega_1\delta_o - \omega_2\delta_3 + \omega_3\delta_2)/2 \\
\dot{\delta}_2 &= (\omega_1\delta_3 + \omega_2\delta_o - \omega_3\delta_1)/2 \\
\dot{\delta}_3 &= (-\omega_1\delta_2 + \omega_2\delta_1 + \omega_3\delta_o)/2 \\
\dot{\omega}_1 &= (-H_{b_3}(\delta)\omega_2 + H_{b_2}(\delta)\omega_3)/(I_1 - J_a) - \lambda_1/(I_1 - J_a)^2 \\
\dot{\omega}_2 &= (-H_{b_1}(\delta)\omega_3 + H_{b_3}(\delta)\omega_1)/(I_2 - J_a) - \lambda_2/(I_2 - J_a)^2 \\
\dot{\omega}_3 &= (-H_{b_2}(\delta)\omega_1 + H_{b_1}(\delta)\omega_2)/(I_3 - J_a) - \lambda_3/(I_3 - J_a)^2
\end{aligned} \tag{8.59}$$

Before proceeding to the co-state equations, the derivatives of H_{b_i} with respect to δ_j are explicitly obtained from Eq. 8.48 as the 3 x 4 matrix

$$\left[\frac{\partial H_{b_i}}{\partial \delta_j}\right] = 2H \begin{bmatrix} \delta_3 & \delta_2 & \delta_1 & \delta_o \\ \delta_o & -\delta_1 & \delta_2 & -\delta_3 \\ -\delta_1 & \delta_o & \delta_3 & \delta_2 \end{bmatrix} \tag{8.60}$$

Co-State Equations

The γ_j co-state equations follow from $\frac{\partial H_1}{\partial \delta_j}$, $j = 1,2,3$, as

$$\dot{\gamma}_o = (-\omega_1\gamma_1 - \omega_2\gamma_2 - \omega_3\gamma_3)/2 + 2H[-\frac{\lambda_1}{(I_1-J_a)}(\delta_1\omega_2 + \delta_o\omega_3) - \frac{\lambda_2}{(I_2-J_a)}(-\delta_3\omega_3 - \delta_1\omega_1) - \frac{\lambda_3}{(I_3-J_a)}(-\delta_o\omega_1 + \delta_3\omega_2)] \tag{8.61a}$$

$$\dot{\gamma}_1 = (\omega_1\gamma_o - \omega_2\gamma_3 + \omega_3\gamma_2)/2 + 2H[-\frac{\lambda_1}{(I_1-J_a)}(\delta_o\omega_2 - \delta_1\omega_3) - \frac{\lambda_2}{(I_2-J_a)}(-\delta_2\omega_3 - \delta_o\omega_1) - \frac{\lambda_3}{(I_3-J_a)}(\delta_1\omega_1 + \delta_2\omega_2)] \tag{8.61b}$$

$$\dot{\gamma}_2 = (\omega_1\gamma_3 + \omega_2\gamma_o - \omega_3\gamma_1)/2 + 2H[-\frac{\lambda_1}{(I_1-J_a)}(-\delta_3\omega_2 + \delta_2\omega_3) - \frac{\lambda_2}{(I_2-J_a)}(-\delta_1\omega_3 + \delta_3\omega_1) - \frac{\lambda_3}{(I_3-J_a)}(-\delta_2\omega_1 + \delta_1\omega_2)] \tag{8.61c}$$

$$\dot{\gamma}_3 = (-\omega_1\gamma_2 + \omega_2\gamma_1 + \omega_3\gamma_o)/2 + 2H[-\frac{\lambda_1}{(I_1-J_a)}(-\delta_2\omega_2 - \delta_3\omega_3) - \frac{\lambda_2}{(I_2-J_a)}(-\delta_o\omega_3 + \delta_2\omega_1) - \frac{\lambda_3}{(I_3-J_a)}(\delta_3\omega_1 + \delta_o\omega_2)] \tag{8.61d}$$

The λ_j co-state equations follow from $\frac{\partial H_1}{\partial \omega_j}$, $j = 0,1,2,3$, as

$$\dot{\lambda}_1 = (\gamma_o\delta_1 - \gamma_1\delta_o - \gamma_2\delta_3 + \gamma_3\delta_2)/2 - \frac{\lambda_2}{(I_2-J_a)} H_{b_3} + \frac{\lambda_3}{(I_3-J_a)} H_{b_2} \tag{8.61e}$$

$$\dot{\lambda}_2 = (\gamma_0\delta_2 + \gamma_1\delta_3 - \gamma_2\delta_0 - \gamma_3\delta_1)/2 + \frac{\lambda_1}{(I_1-J_a)} H_{b_3}$$

$$- \frac{\lambda_3}{(I_3-J_a)} H_{b_1} \tag{8.61f}$$

$$\dot{\lambda}_3 = (\gamma_0\delta_3 - \gamma_1\delta_2 + \gamma_2\delta_1 - \gamma_3\delta_0)/2 - \frac{\lambda_1}{(I_1-J_a)} H_{b_2}$$

$$+ \frac{\lambda_2}{(I_2-J_a)} H_{b_1} \tag{8.61g}$$

Necessary Conditions for Minimizing J_2

The necessary conditions are obtained in a fashion similar to that described above with the exception that the torques (u_i) are treated as additional state variables instead of controls, as follows.

We define three new pseudo states (u_i) given by the following differential equations

$$\frac{d}{dt}(u_i) = \dot{u}_i = \bar{u}_i \quad , \quad i = 1,2,3 \tag{8.62}$$

where $\bar{u}_i$, i = 1,2,3 are the "controls". Next the Hamiltonian is written as

$$H_2 = \frac{1}{2}\sum_{i=1}^{3} \bar{u}_i^2 + \sum_{i=0}^{3} \gamma_i\dot{\delta}_i + \sum_{i=1}^{3} \lambda_i\dot{\omega}_i + \sum_{i=1}^{3} c_i\dot{u}_i \tag{8.63}$$

where c_i are additional co-states, and we must substitute Eqs. 8.59, 8.62 to eliminate $\dot{\delta}_i$, $\dot{\omega}_i$, $\dot{u}_i$ to obtain the explicit equation for the Hamiltonian H_2.

The extremality of H_2 leads to the following choice for $\bar{u}_i$:

$$\frac{\partial H_2}{\partial \bar{u}_i} = 0 = \bar{u}_i + c_i \rightarrow \bar{u}_i = - c_i \quad , \quad i = 1,2,3 \tag{8.64}$$

The state, co-state equations are derived following an analogous process as in Eqs. 8.59 through 8.61.

The first four state ($\delta_0,\delta_1,\delta_2,\delta_3$) differential equations in Eq. 8.59 remain unaltered. Equation 8.62 for u_i are rewritten by eliminating $\bar{u}_i$ as

$$\dot{u}_i = - c_i \quad , \quad i = 1,2,3 \tag{8.65}$$

The first seven co-state equations in Eq. 8.61 remain unaltered. New co-state equations for c_i are given by

$$\dot{c}_i = -\frac{\partial H_2}{\partial u_i} = -\lambda_i \frac{\partial(\dot{\omega}_i)}{\partial u_i} = \lambda_i/(I_i - J_a) \quad , \quad i = 1,2,3 \tag{8.66}$$

Arbitrary boundary conditions can now be prescribed on u_i (i.e., $u_i(0)$ and $u_i(T)$). The number of states and co-states increase from seven to ten.

Necessary Conditions for Minimizing J_3

We define three pseudo states ($\dot{u}_i = \bar{u}_i$) in addition to u_i such that

$$\frac{d}{dt}(\bar{u}_i) = \frac{d^2}{dt^2} u_i = \ddot{\bar{u}}_i \quad , \quad i = 1,2,3 \tag{8.67}$$

and we take $\ddot{\bar{u}}_i = \dddot{u}_i$ as the control variables.

The Hamiltonian

$$H_3 = \frac{1}{2} \sum_{i=1}^{3} \ddot{\bar{u}}_i^2 + \sum_{i=0}^{3} \gamma_i \dot{\delta}_i + \sum_{i=1}^{3} \lambda_i \dot{\omega}_i$$

$$+ \sum_{i=1}^{3} c_i \dot{u}_i + \sum_{i=1}^{3} d_i \dot{\bar{u}}_i \tag{8.68}$$

where d_i are three additional co-states.

The controls ($\ddot{\bar{u}}_i$) extremizing H_3 are such that

$$\frac{\partial H_3}{\partial \ddot{\bar{u}}_i} = 0 = \ddot{\bar{u}}_i + d_i \quad , \quad i = 1,2,3 \tag{8.69}$$

this yields

$$\ddot{\bar{u}}_i = -d_i \quad , \quad i = 1,2,3$$

The first seven state ($\delta_0, \delta_1, \delta_2, \delta_3, \omega_1, \omega_2, \omega_3$) equations are the same as in Eq. 8.59. The equations for u_i are given as

$$\dot{u}_i = \bar{u}_i \quad , \quad i = 1,2,3 \tag{8.70}$$

Using Eq. 8.69, the equations for $\dot{\bar{u}}_i$ are rewritten as

$$\dot{\bar{u}}_i = -d_i \quad , \quad i = 1,2,3 \tag{8.71}$$

The first ten co-state equations are the same as Eqs. 8.61 and 8.66. The new co-state equations for d_i are given by

$$\dot{d}_i = -\frac{\partial H_3}{\partial \bar{u}_i} = -c_i \quad , \quad i = 1,2,3 \tag{8.72}$$

The number of states and co-states increase from ten to thirteen. We are now in a position to prescribe boundary conditions on u_i and $\dot{u}_i$. This is a form of torque shaping and permits zero control and control rates to be constrained initially and finally. Such maneuvers are not only smoother at interior times, they are also constrained to start and stop with prescribed values and slopes and, as a consequence, excite flexural degrees of freedom of the spacecraft to a lesser degree. In Chapter 10, we generalize these concepts to explicitly suppress vibration of flexible appendages and demonstrate conclusively the importance of control derivative penalties in suppression of vibration during large-angle maneuvers.

8.4.3 An Example Maneuver: De-Tumble With Momentum Transfer

A class of more general reorientation (than the 1-wheel momentum transfer of Section 8.2) and detumble maneuvers can be performed by the three-wheel configuration depicted in Fig. 8.10. We consider one such maneuver and show the effect of different performance indices of the previous section on the control torque and state histories. The spacecraft parameters are the same as before; the boundary conditions are given below.

	Initial Conditions ($t_o = 0$)	Final Conditions ($t_f = T = 100$ sec.)
β_0	.64278761	1
β_1	.44227597	0
β_2	.44227597	0
β_3	.44227597	0
ω_1	.01 r/s	0
ω_2	.005 r/s	0
ω_3	.001 r/s	0
Ω_1	0	H_{n1}/J_a
Ω_2	0	H_{n2}/J_a
Ω_3	0	H_{n3}/J_a

The initial conditions correspond to an arbitrarily tumbling state, with the wheels locked and an instantaneous attitude such that the initial direction cosines of the principal line $\hat{\ell}_{n_b}$ are $(1/\sqrt{3}, 1/\sqrt{3}, 1/\sqrt{3})$ and the principal rotation angle ϕ_{n_b} is 100°. The final conditions require nulling of the spacecraft angular rates and reorientation such that the body axes become coincident with the inertial frame. The wheel speeds at the final time can be determined in general by

$$\Omega_i = (H_{b_i}(\delta) - I_i\omega_i)/J_a \tag{8.73}$$

The body axes components of the angular momentum vector at the initial time are computed as:

$$H_{b_1}(0) = .86315,\ H_{b_2}(0) = .42585,\ H_{b_3}(0) = .113665$$

The inertial components of the momentum vector are computed by using the transformation

$$\{\mathbf{H}_n\} = [C(\beta(0))]^T\{\mathbf{H}_b(0)\} \tag{8.74}$$

Knowing $H_{b_i}(0)$ and $\beta_i(0)$, the constant inertial angular momentum components

H_{n_i} are computed:

$$H_{n_1} = .221359,\ H_{n_2} = .900938,\ H_{n_3} = .280368$$

This permits numerical calculation of the final wheel speeds as

$$\begin{Bmatrix} \Omega_1 \\ \Omega_2 \\ \Omega_3 \end{Bmatrix}_{t_f} = \frac{1}{J_a} \begin{Bmatrix} H_{n_1} \\ H_{n_2} \\ H_{n_3} \end{Bmatrix} = \begin{Bmatrix} 4.42718 \\ 18.01876 \\ 5.6036 \end{Bmatrix}$$

Next α_i are calculated from Eq. 8.46b. Note for the present example, α_i and $\delta_i(T)$ are the same; we complete the following values:

$$\alpha_0 = .982241,\ \alpha_1 = -.147258,\ \alpha_2 = 0,\ \alpha_3 = .116265$$

Finally the $\delta_i(0)$ are are computed from Eq. 8.47.

Now we are in a position to impose the required boundary conditions. The Euler parameters are constrained by the exact integral $\Sigma_{i=0}^{3}\beta_i^2 = 1$ implicit in Eq. 8.41. Hence the boundary condition on $\beta_0(T)$ is not imposed explicitly. The Method of Particular Solutions (Chapter 7, Ref. 15) was applied, starting simply with a linear function of time assumed for each state variable to connect the initial and final states (as the starting iteration). Even with this crude trial trajectory we successfully converged to optimal numerical solution for the three trajectories corresponding to minimization of the performance indices J_1, J_2, and J_3 respectively. The number of iterations required and the values of the performance indices are given below:

Performance Index	No. of Iterations	Performance Index J_i	Energy Index (E)
J_1	6	.248039(N^2m^2s)	229.457 (J)
J_2	5	.001477(N^2m^2/s^2)	346.501 (J)
J_3	5	.000021 (N^2m^2/s^3)	463.682 (J)

From Fig. 8.11 we see that the torques for J_1 are non-zero at both the initial and final times. Implementation of this control would make the spacecraft

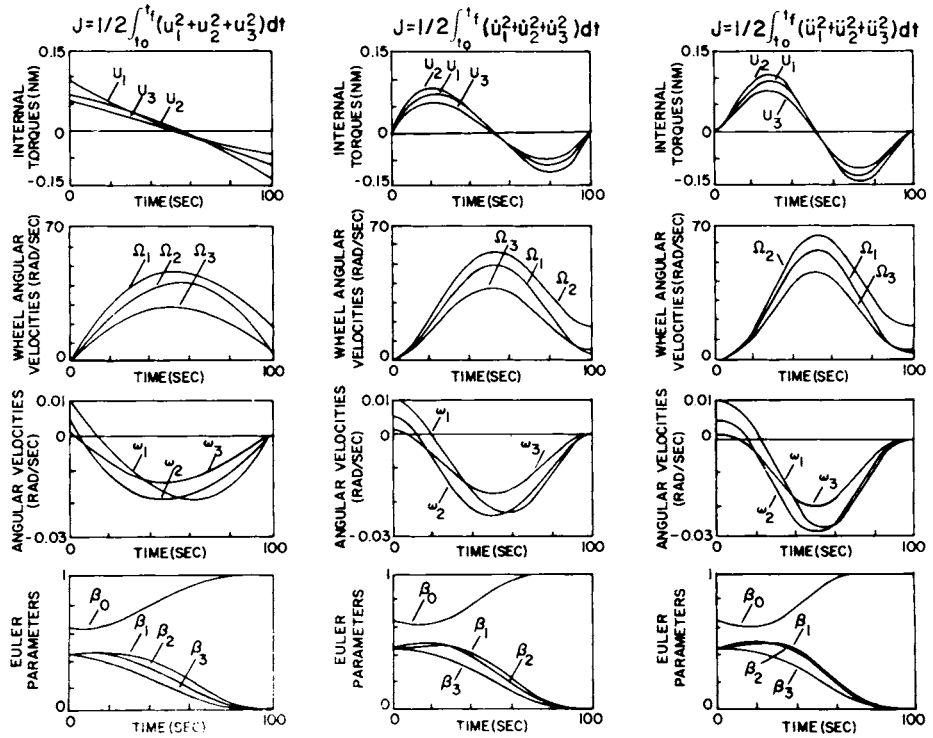

Figure 8.11 Three Optimal Momentum Transfer Maneuvers: Effect of Control Derivative Penalties in the Performance Index

start and stop with jerks, which is undesirable, especially for large fragile vehicles. The second and third column of Figure 8.11 (for J_2, J_3) shows the effects of imposing boundary conditions on the control and it's derivatives respectively. The smooth maneuvers produced by these torques can be seen from the trajectories of the states. Notice that imposing boundary conditions of this nature increases the peak control torque requirements, and also increases the peak angular velocities of the spacecraft and the wheel speeds at intermediate points considerably. The energy requirements increase almost linearly with the constraints imposed on the controls.

A further generalization of the above formulations leads to a performance index of the form

$$J_4 = \frac{1}{2}\int_0^T \sum_{j=1}^{3} [w_{1j}u_j^2 + w_{2j}\dot{u}_j^2 + w_{3j}\ddot{u}_j^2]dt \tag{8.75}$$

However, unless the weights w_{1j} and w_{2j} are small compared to w_{3j}, the TPBVP constitutes a system of stiff differential equations which we found difficult to solve by Runge-Kutta methods.

8.5 OPTIMAL LARGE ANGLE MANEUVERS OF A SINGLE RIGID BODY

8.5.1 Introductory Remarks

Here we consider external torque optimal maneuvers of a single rigid body in order to illustrate a useful *boundary condition continuation* method for solving nonlinear TPBVP. These maneuvers are quite general three dimensional large angular motions where the nonlinear kinematic and dynamic coupling effects are included. Unlike the momentum transfer maneuvers of the forgoing developments, we are now prepared to impose general three dimensional constraints upon both the attitude and angular velocity, both initially and finally.

8.5.2 Kinematics and Dynamics

Using results of Chapters 2-4, we begin by defining two reference frames: $\{\hat{b}\} = [\hat{b}_1\hat{b}_2\hat{b}_3]^T$, an orthonormal set of unit vectors oriented along the space vehicle's principal axes; and $\{\hat{n}\} = [\hat{n}_1\hat{n}_2\hat{n}_3]^T$, an orthonormal set of unit vectors arbitrarily oriented, but fixed in inertial space. The relative orientation of the vehicle to the inertial axes is defined by

$$\{\hat{b}\} = [C]\{\hat{n}\} \tag{8.76}$$

where [C] is the direction cosine matrix. In lieu of any three-angle description or orientation, we adopt the four Euler parameters defined as

$$\beta_0 = \cos(\phi/2) \quad , \quad \beta_i = \ell_i \sin(\phi/2) \quad , \quad i = 1,2,3 \tag{8.77}$$

and

$$\beta \triangleq [\beta_0 \quad \beta_1 \quad \beta_2 \quad \beta_3]^T$$

where

$$\hat{\ell} \equiv \ell_1\hat{n}_1 + \ell_2\hat{n}_2 + \ell_3\hat{n}_3 \equiv \ell_1\hat{b}_1 + \ell_2\hat{b}_2 + \ell_3\hat{b}_3$$

is the principal vector, and ϕ is the principal angle. Inspection of Eq. 8.77 reveals the β's satisfy the constraint

$$\sum_{i=0}^{3} \beta^2 = 1 \tag{8.78}$$

The existence of $\hat{\ell}$ and ϕ, corresponding to arbitrary admissible values for the elements of [C], is guaranteed by Euler's Principal Rotation Theorem (Section 2.5).

The direction cosine matrix can be parameterized as a function of Euler parameters as (see Chapter 2)

$$[C] = \begin{bmatrix} (\beta_0^2+\beta_1^2-\beta_2^2-\beta_3^2) & 2(\beta_1\beta_2+\beta_0\beta_3) & 2(\beta_1\beta_3-\beta_0\beta_2) \\ 2(\beta_1\beta_2-\beta_0\beta_3) & (\beta_0^2-\beta_1^2+\beta_2^2-\beta_3^2) & 2(\beta_2\beta_3+\beta_0\beta_1) \\ 2(\beta_1\beta_3+\beta_0\beta_2) & 2(\beta_2\beta_3-\beta_0\beta_1) & (\beta_0^2-\beta_1^2-\beta_2^2+\beta_3^2) \end{bmatrix} \tag{8.79}$$

The Euler parameters' time derivatives are rigorously related to the angular velocity $\omega = (\omega_1\omega_2\omega_3)^T$ of $\{\hat{b}\}$ relative to $\{\hat{n}\}$ via the orthogonal kinematic relationship (see Eqs. 2.74 and 2.75).

$$\dot{\beta} = [\underline{\Omega}]\beta = [\underline{\beta}]\omega \tag{8.80}$$

where

$$\underline{\Omega} = \frac{1}{2}\begin{bmatrix} 0 & -\omega_1 & -\omega_2 & -\omega_3 \\ \omega_1 & 0 & \omega_3 & -\omega_2 \\ \omega_2 & -\omega_2 & 0 & \omega_1 \\ \omega_3 & \omega_2 & -\omega_1 & 0 \end{bmatrix}$$

$$\underline{\dot{\beta}} = \frac{1}{2}\begin{bmatrix} -\beta_1 & -\beta_2 & -\beta_3 \\ \beta_0 & -\beta_3 & \beta_2 \\ \beta_3 & \beta_0 & -\beta_1 \\ -\beta_2 & \beta_1 & \beta_0 \end{bmatrix}$$

Equation 8.80 presents a sharp contrast to the corresponding kinematical relationship for any three-angle description of orientation (which invariably contains ratios of transcendental functions of the angles, and has a geometric singularity in which two of the three angular rates tend to infinity for finite ω_i). Equation 8.80 has an implicit, exact integral $\sum_{i=0}^{3} \beta_i^2$ = constant. As is evident from Eq. 8.78, this constant should be unity, and is established by any valid choice of initial conditions.

8.5.3 Optimal Maneuver Necessary Conditions

To consider the rotational dynamics of a rigid space vehicle, we choose as state variables the four Euler parameters $(\beta_0,\beta_1,\beta_2,\beta_3)$ and the angular velocities $(\omega_1,\omega_2,\omega_3)$; the state differential equations are thus Eq. 8.80 together with Euler's rotational equations of motion

$$\dot{\omega} = f(\omega) + Du \tag{8.81}$$

where

$$f = (-g_1\omega_2\omega_3,\ -g_2\omega_1\omega_3,\ -g_3\omega_1\omega_2)^T$$

$$D = \begin{bmatrix} I_1^{-1} & 0 & 0 \\ 0 & I_2^{-1} & 0 \\ 0 & 0 & I_3^{-1} \end{bmatrix}$$

where I_1, I_2, and I_3 are the spacecraft principal inertias, u_1, u_2, and u_3 are $\hat{\mathbf{b}}_i$ components of the control torque, and $g_1 \equiv (I_3-I_2)/I_1$, $g_2 \equiv (I_1-I_3)/I_2$, $g_3 \equiv (I_2 - I_1)/I_3$. We seek a solution of Eqs. 8.80 and 8.81, satisfying the prescribed initial and final orientation and angular velocity given by

$$\beta_i(t_o) = \beta_{io}, \ \omega_j(t_o) = \omega_{jo} \quad , \quad \beta_i(t_f) = \beta_{if}, \ \omega_j(t_f) = \omega_{jf}$$
$$(i = 0,1,2,3; \quad j = 1,2,3) \tag{8.82}$$

Observe that the prescription of Euler parameter boundary conditions must be consistent with the constraint (see Eq. 8.78) so that only 12 degrees of freedom exist.

We seek, in particular, the torque history $u_i(t)$ generating an optimal solution of Eqs. 8.80 and 8.81, satisfying the boundary conditions of Eq. 8.82, and which minimizes the performance index

$$J = \frac{1}{2}\int_{t_o}^{t_t} [u_1^2(t) + u_2^2(t) + u_3^2(t)]dt \tag{8.83}$$

We restrict attention to a piecewise continuous torque history $u_i(t)$.

The Hamiltonian function associated with minimizing Eq. 8.83 along trajectories of Eqs. 8.80 and 8.81 is

$$H = 1/2\mathbf{u}^T\mathbf{u} + \boldsymbol{\gamma}^T\underline{\underline{\beta}}\,\boldsymbol{\omega} + \boldsymbol{\lambda}^T(\mathbf{f}(\boldsymbol{\omega}) + D\mathbf{u}) \tag{8.84}$$

where λ_i and γ_j are co-state variables associated with β_i and ω_j. In addition to Eqs. 8.80 and 8.81, Pontryagin's Principle requires as necessary conditions that the λ's and γ's satisfy co-state differential equations derivable from

$$\dot{\boldsymbol{\gamma}} = -(\partial H/\partial \boldsymbol{\beta})^T = \underline{\underline{\Omega}}\,\boldsymbol{\gamma} \tag{8.85}$$

and

$$\dot{\boldsymbol{\lambda}} = -(\partial H/\partial \boldsymbol{\omega})^T = -(\partial \mathbf{f}/\partial \boldsymbol{\omega})^T\boldsymbol{\lambda} - \underline{\underline{\beta}}^T\boldsymbol{\gamma}$$

where we have made use of the fact that $\underline{\underline{\Omega}} = -\underline{\underline{\Omega}}^T$, and $u_j(t)$ must be chosen at every instant so that the Hamiltonian H is minimized. This latter necessary condition requires (for $u_i(t)$ continuous and unbounded) that

$$\partial H/\partial u_i = 0 = u_i + \lambda_i/I_i \quad , \quad i = 1,2,3$$

the optimal torque vector is

$$u_i = -\lambda_i/I_i \quad , \quad i = 1,2,3 \tag{8.86}$$

The state and co-state differential equations forming the boundary value problem are Eqs. 8.80 and 8.81 after using Eq. 8.86, together with the co-state equations.

State Equations

$$\dot{\beta} = \underline{\underline{\Omega}}\,\beta \tag{8.87a}$$

$$\dot{\omega} = \mathbf{f}(\omega) - DD\lambda \tag{8.87b}$$

Co-State Equations

$$\dot{\gamma} = \underline{\underline{\Omega}}\,\gamma \tag{8.87c}$$

$$\dot{\lambda} = -(\partial \mathbf{f}/\partial\omega)^T\lambda - \beta^T\gamma \tag{8.87d}$$

The next two sections deal with initializing and completion of a continuation process for determination of the generally unknown $\gamma_i(t_o)$ and $\lambda_i(t_o)$ for the solution of the boundary-value problem. This process takes full account of the fact that

$$\sum_{i=0}^{3} \gamma_i^2(t) = \text{const}$$

is a rigorous integral of Eq. 8.87c, however unlike Euler parameters, the constant cannot be taken as unity. This fact will be evident in the following developments.

8.5.4 Analytical Solution for a Special Case: Single Axis Maneuvers

In general Eqs. 8.87 does not admit analytical solutions, and numerical solutions must be iterated to achieve satisfaction of the terminal boundary conditions. However, certain boundary conditions zero certain terms of Eq. 8.87 for all time, and thereby (without approximation) reduce them to specialized forms which can be solved analytically. Implicit special case solutions for the initial co-state boundary conditions are then achievable *without* iteration. These initial conditions will then be used to start an

iterative relaxation (continuation or homotopy) process to solve the more general maneuver problems.

The three special case solutions correspond to "pure spin" (or "single axis") reorientations about any one of the spacecraft's three principal axes of inertia. The corresponding boundary conditions for rotation about the ith axes are:

$$\begin{aligned} \beta_0(t_0) &= \cos(\phi_0/2) & \beta_j(t_0) &= \sin(\phi_0/2)\delta_{ji} \\ \beta_0(t_f) &= \cos(\phi_f/2) & \beta_j(t_f) &= \sin(\phi_f/2)\delta_{ji} \\ \omega_k(t_0) &= \dot{\phi}_0\delta_{ki} & \omega_k(t_f) &= \dot{\phi}_f\delta_{ki} \end{aligned} \qquad (8.88)$$

$$(j = 1,2,3;\ k = 1,2,3)$$

where δ_{ij} is the Kronecker delta symbol

$$\delta_{ij} = \begin{cases} 0 & , \quad i \neq j \\ 1 & , \quad i = j \end{cases}$$

In all three cases, the initial angle ϕ_0, initial angular rate $\dot{\phi}_0$, final angle ϕ_f, and final angular rate $\dot{\phi}_f$ can be given arbitrary values. Except for the use of the Euler Parameters, these single axis measures are in fact physically identical to the maneuvers of Section 6.4. For example, we consider in detail the case of i = 1. It can be seen by inspection that the 14 differential equations implicit in the vector equations of Eq. 8.87 reduce to

$$\begin{aligned} \dot{\beta}_0 &= -(\omega_i/2)\beta_i & \dot{\beta}_1 &= (\omega_1/2)\beta_0 & \dot{\beta}_2 &= \dot{\beta}_3 = 0 \\ \dot{\omega}_1 &= -\lambda_1/I_1^2 & \dot{\omega}_2 &= \dot{\omega}_3 = 0 & & \\ \dot{\gamma}_0 &= -(\omega_1/2)\gamma_1 & \dot{\gamma}_1 &= (\omega_1/2)\gamma_0 & \dot{\gamma}_2 &= \dot{\gamma}_3 = 0 \\ \dot{\lambda}_1 &= 1/2(\gamma_0\beta_1 - \gamma_1\beta_0) & \dot{\lambda}_2 &= \dot{\lambda}_2 = 0 & & \end{aligned} \qquad (8.89)$$

which have the solutions

$$\beta_0(t) = \cos(\phi/2) \qquad \beta_1(t) = \sin(\phi/2) \qquad \beta_2(t) = \beta_3(t) = 0$$

$$\gamma_0(t) = -2I_1^2\dddot{\phi}_0\sin(\phi/2) \qquad \gamma_1(t) = 2I_1^2\dddot{\phi}_0\cos(\phi/2) \qquad \gamma_2(t) = \gamma_3(t) = 0$$

$$\phi(t) = \phi_0 + \dot{\phi}_0(t - t_0) + 1/2\ddot{\phi}_0(t - t_0)^2 + 1/6\dddot{\phi}_0(t - t_0)^3$$

$$\omega_1(t) = \dot{\phi}(t) \qquad \omega_2(t) = \omega_3(t) = 0$$

$$\ddot{\phi}_0 = \frac{6(\phi_f-\phi_0)}{(t_f-t_0)^2} - \frac{2(2\dot{\phi}_0+\dot{\phi}_f)}{(t_f-t_0)}$$

$$\dddot{\phi}_0 = -\frac{12(\phi_f-\phi_0)}{(t_f-t_0)^3} + \frac{6(\dot{\phi}_0+\dot{\phi}_f)}{(t_f-t_0)^2}$$

$$\lambda_1(t) = -I_1^2\ddot{\phi}_0 - I_1^2\dddot{\phi}_0(t - t_0) \quad , \quad \lambda_2(t) = \lambda_3(t) = 0$$

$$u_1(t) = -\lambda_1(t)/I_1 = I_1[\ddot{\phi}_0 + \dddot{\phi}_0(t - t_0)] = I_1\dot{\omega}_1$$

$$u_2(t) = u_3(t) = 0 \qquad (8.90)$$

The key point of interest in the solutions just presented comes in the evaluation of the free constants in the equation for λ_1. It was determined (Ref. 17) that the norm ($\gamma^T(t)\gamma(t) = B$ = constant) for the angular velocity costate is not unique, but is bounded below by a positive constant. This truth motivates the formulation of the differential correction algorithm of Section 8.5.5 based upon the strategy that the magnitude of the angular velocity costate be minimized.

The results just stated for i = 1 can be quickly paralleled to produce solution for i = 2,3:

$$\gamma_0(t_0) = -2I_i^2\ddot{\phi}_0\beta_i(t_0) \quad \gamma_i(t_0) = -2I_i^2\dddot{\phi}_0\beta_0(t_0)$$

$$\gamma_k(t_0) = 0 \quad (k \neq 1 \quad , \quad k = 1,2,3)$$

$$\lambda_i(t_0) = -I_i^2\ddot{\phi}_0 \quad \lambda_k(t_0) = 0 \quad (k \neq i \quad ; \quad i = 1,2,3)$$

$\phi_0, \dot{\phi}_0, \phi_f, \dot{\phi}_f$, given $\ddot{\phi}_0, \dddot{\phi}_0$ are found from Eq. 8.90.

8.5.5 A Continuation Process for Solution of the Two-Point Boundary-Value Problem

We now consider a continuation process for solution of the nonlinear two-point boundary-value problem; the initial step is to select, as a starting

iterative, one of the above analytical solutions for pure spin about a principal axis (based, for example, upon which axis has the largest initial or final angular velocity component). The continuation process is nonstandard in that it is carried out in the space of terminal boundary conditions (rather than, for example, introducing a family parameter directly into the differential equations). The continuation process defines a family of neighboring boundary-value problems; the first in the sequence being analytically solvable and the final being the actual desired boundary-value problem. The intermediate problems are merely stepping stones which allow neighboring optimal trajectories' converged co-states to be employed as starting iteratives. By adaptively controlling the size of the continuation steps, we provide "arbitrary close" starting iteratives which ensure the validity of the linearity assumption in the Newton iteration process.

One problem encountered when using the Euler parameter representation is that these parameters are redundant by virtue of the constraint (see Eq. 8.78). We must therefore be careful in constructing algorithms for solving the two-point boundary-value problem. The redundancy of the β's evident in Eq. 8.78 results in a corresponding redundancy in the co-state variables. Since the γ's satisfy a skew symmetric differential equation (Eq. 8.87c) identical to the β's differential equation (Eq. 8.87a), it is evident that

$$\gamma_0^2(t) + \gamma_1^2(t) + \gamma_2^2(t) + \gamma_3^2(t) = \text{const} = B^2 \tag{8.91}$$

We have seen already that B is bounded below, although it is not unique. The fact that the initial γ's must, in general, be iteratively determined, motivates choosing some well-defined process for selecting a particular solution. To this end, "it seems altogether reasonable" to approach the general solution analogous to the approach of References 16, 17; we determine the initial co-state boundary conditions $\lambda_i(t)$ and $\gamma_i(t_o)$ which satisfy $\beta_i(t_f) = \beta_{if}$ and $\omega_i(t_f) = \omega_{if}$, with the criterion that

$$B^2 = \sum_{j=0}^{3} \gamma_j^2(t_o)$$

be minimized.

Since the terminal Euler parameters must satisfy Eq. 8.78, it is necessary to formally constrain only three of $\beta_i(t_f) = \beta_{if}$, where $i = 0,1,2,3$; the remaining $\beta_i(t_f)$ will automatically satisfy Eq. 8.78 (by virtue of the fact that Eq. 8.78, is satisfied by any admissible initial state, and the skew symmetric differential Eq. 8.87a has $\Sigma\beta_i^2$ = constant as a rigorous exact integral). These considerations motivate a successive approximation strategy to solve the two-point boundary-value problem as follows:

Given starting estimates for the co-state vectors

$$\hat{\gamma}(t_o) = [\hat{\gamma}_o(t_o),\hat{\gamma}_1(t_o),\hat{\gamma}_2(t_o),\hat{\gamma}_3(t_o)]^T$$
$$\hat{\lambda}(t_o) = [\hat{\lambda}_1(t_o),\hat{\lambda}_2(t_o),\hat{\lambda}_3(t_o)]^T$$

we seek correction vectors $\Delta\gamma$ and $\Delta\lambda$ which minimize

$$B^2 = [\hat{\gamma}(t_o) + \Delta\gamma]^T[\hat{\gamma}(t_o) + \Delta\gamma]$$
$$= \hat{\gamma}_o(t_o)^T\hat{\gamma}(t_o) + 2\Delta\gamma^T\hat{\gamma}(t_o) + \Delta\gamma^T\Delta\gamma \qquad (8.92a)$$

subject to the terminal constraints

$$\beta_f' - \beta'[\hat{\gamma}(t_o) + \Delta\gamma,\ \hat{\lambda}(t_o) + \Delta\lambda,\ t_f] = 0$$
$$\omega_f - \omega[\hat{\gamma}(t_o) + \Delta\gamma,\ \hat{\lambda}(t_o) + \Delta\lambda,\ t_f] = 0 \qquad (8.92b)$$

where

$$\beta'(t) = [\beta_1(t),\beta_2(t),\beta_3(t)]^T \quad , \quad \omega(t) = [\omega_1(t),\omega_2(t),\omega_3(t)]^T$$
$$\beta_f' = \beta(t_f) \quad , \quad \omega_f = \omega(t_f)$$

Assuming some process has led to specific fixed values for the initial β's and ω's, we proceed to develop a differential correction process for $\Delta\gamma$ and $\Delta\lambda$.

Linearizing Eq. 8.92, we have

$$\beta_f - \hat{\beta} - A_{\beta\gamma}\Delta\gamma - A_{\beta\lambda}\Delta\lambda = 0 \qquad (8.93a)$$
$$\omega_f - \hat{\omega} - A_{\omega\gamma}\Delta\gamma - A_{\omega\lambda}\Delta\lambda = 0 \qquad (8.93b)$$

where $\hat{\beta}' \equiv \beta'[\hat{\gamma}(t_0), \hat{\lambda}(t_0), t_f]$ and $\hat{\omega} \equiv \omega[\hat{\gamma}(t_0), \hat{\lambda}(t_0)t_f]$ represent the solution of Eq. 8.87 based upon the current estimate $\hat{\gamma}(t_0)$ and $\hat{\lambda}(t_0)$ of the initial co-state.

$$A_{\beta\gamma} \equiv \frac{\partial\beta'[\hat{\gamma}(t_0),\lambda(t_0),t_f]}{\partial[\gamma(t_0)]}\bigg|_{\hat{\gamma}(t_0),\hat{\lambda}(t_0)} = \frac{\partial\beta_f'}{\partial\gamma_0} \tag{8.94a}$$

$$A_{\beta\lambda} \equiv \frac{\partial\beta'[\gamma(t_0),\lambda(t_0),t_f]}{\partial[\lambda(t_0)]}\bigg|_{\hat{\gamma}(t_0),\hat{\lambda}(t_0)} = \frac{\partial\beta_f'}{\partial\lambda_0} \tag{8.94b}$$

$$A_{\omega\gamma} = \frac{\partial\omega[\gamma(t_0),\lambda(t_0),t_f]}{\partial[\gamma(t_0)]}\bigg|_{\hat{\gamma}(t_0),\hat{\lambda}(t_0)} = \frac{\partial\omega_f}{\partial\gamma_0} \tag{8.94c}$$

$$A_{\omega\lambda} = \frac{\partial\omega[\gamma(t_0),\lambda(t_0),t_f]}{\partial[\lambda(t_0)]}\bigg|_{\hat{\gamma}(t_0),\hat{\lambda}(t_0)} = \frac{\partial\omega_f}{\partial\lambda_0} \tag{8.94d}$$

The calculation of these derivatives is a separate issue, dealt with in Appendix 1 of Reference 17.

Observe that Eq. 8.92a, to be minimized, does not explicitly depend upon $\Delta\lambda$, but $\Delta\gamma$ and $\Delta\lambda$ are constrained by Eq. 8.93; thus $\Delta\lambda$ cannot be assigned arbitrary values. Since $A_{\omega\lambda}$ is square and presumed to be nonsingular, we can determine $\Delta\lambda$ from Eq. 8.93b as a function of $\Delta\gamma$ by

$$\Delta\lambda = A_{\omega\lambda}^{-1}(\omega_f - \hat{\omega}) - A_{\omega\lambda}^{-1}A_{\omega\gamma}\Delta\gamma \tag{8.95}$$

Substitution of Eq. 8.95 into Eq. 8.93a then replaces Eq. 8.93 by a single constraining relationship depending only upon $\Delta\underline{\gamma}$:

$$(\beta_f - \hat{\beta}) - A_{\beta\lambda}A_{\omega\lambda}^{-1}(\omega_f - \hat{\omega}) - \tilde{A}\Delta\gamma = 0 \tag{8.96}$$

where

$$\tilde{A} \equiv A_{\beta\gamma} - A_{\beta\lambda}A_{\omega\lambda}^{-1}A_{\omega\gamma} \tag{8.97}$$

Using the Lagrange multiplier rule to minimize Eq. 8.92a subject to the constraint cited in Eq. 8.96, we introduce the augmented function

$$\Phi = \hat{\gamma}^T(t_0)\hat{\gamma}(t_0) + 2\hat{\gamma}^T(t_0)\Delta\gamma + \Delta\gamma^T\Delta\gamma + \Lambda^T[(\beta_f - \hat{\beta}) - A_{\beta\lambda}A_{\omega\lambda}^{-1}(\omega_f - \hat{\omega}) - \tilde{A}\Delta\gamma] \tag{8.98}$$

where Λ is a 3 x 1 vector of Lagrange multipliers. We seek corrections $\Delta\gamma$ to

the initial co-state which minimize Eq. 8.98; as a necessary condition, we require

$$\frac{\partial \Phi}{\partial(\Delta\gamma)} = 0 = 2\hat{\gamma}(t_o) + 2\Delta\gamma - \bar{A}^T\Lambda \tag{8.99}$$

Since the function (Eq. 7.92) is a positive definite quadratic form, and the constraint of Eq. 8.96 is linear, it follows that sufficient conditions are satisfied, and Φ is uniquely minimized by the stationary point satisfying Eq. 8.99. The optimum $\gamma(t_o)$ corrections, in terms of Λ, follow from Eq. 8.99 as

$$\Delta\gamma = 1/2\bar{A}^T\Lambda - \hat{\gamma}(t_o) \tag{8.100}$$

Substitution of Eq. 8.100 into the constraint of Eq. 8.96 yields a solution for the multipliers as

$$1/2\Lambda = (\bar{A}\bar{A}^T)^{-1}[(\beta_f - \hat{\beta}) - A_{\beta\lambda}A_{\omega\lambda}^{-1}(\omega_f - \hat{\omega}) + \bar{A}\hat{\gamma}(t_o)] \tag{8.101}$$

Substitution of Eq. 8.101 into Eq. 8.100 yields the solution for $\Delta\gamma$ as

$$\Delta\gamma = \bar{A}^T(\bar{A}\bar{A}^T)^{-1}[(\beta_f' - \beta') - A_{\beta\lambda}A_{\omega\lambda}^{-1}(\omega_f - \hat{\omega}) + \bar{A}\hat{\gamma}(t_o)] - \hat{\gamma}(t_o) \tag{8.102}$$

The solution for $\Delta\lambda$ then follows immediately from Eq. 8.95.

This discussion can all be summarized as the differential correction algorithm, shown in Fig. 8.12, for refining given approximate initial co-states $\gamma(t_o)$ and $\lambda(t_o)$ so that a solution is achieved (provided the starting estimates are "sufficiently good").

Let us consider a continuation process which should effectively guarantee that the algorithm of Fig. 8.12 will work reliably. The only significant assumption en route to the algorithm was the local linearization of Eq. 8.92 to obtain Eq. 8.93. Ignoring certain singular events (leading to the inverses in Eqs. 8.93 and 8.102 not existing, these events are associated with bifurcations or turning points), we can expect this algorithm to converge if the starting estimates $\hat{\gamma}(t_o)$ and $\hat{\lambda}(t_o)$ are sufficiently close to their true values. We describe an "adaptive continuation process" in which we can always obtain

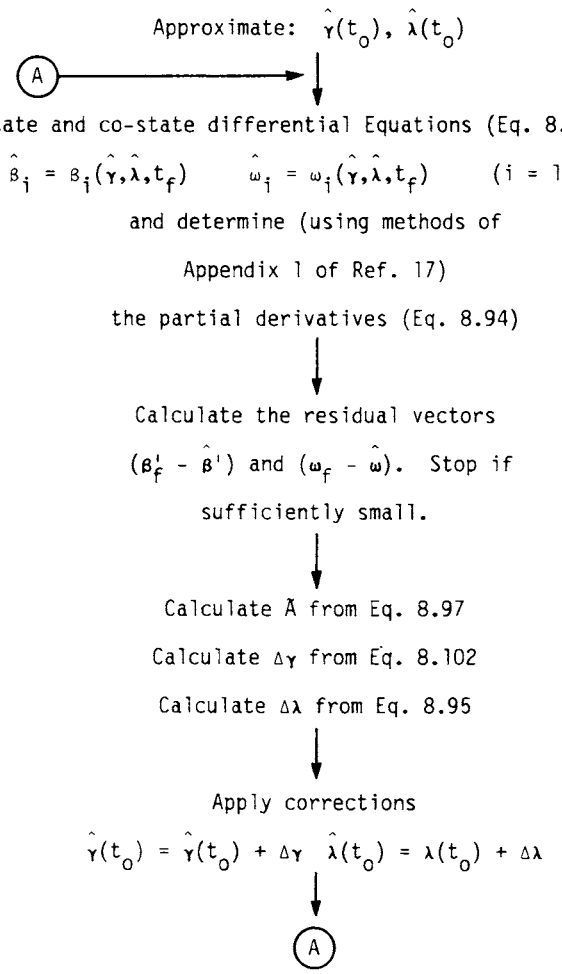

Figure 8.12 Differential correction algorithm for determination of initial co-state variables.

starting estimates with arbitrarily small displacements from their true values.

Use is made of the fact that the necessary conditions can be rigorously satisfied if the boundary conditions belong to either of the three sets defined by Eqs. 8.88. Defining the sequence of boundary conditions

$$X_n = [\theta_{1n}(t_o),\theta_{2n}(t_o),\theta_{3n}(t_o),\omega_{1n}(t_o),\omega_{2n}(t_o),\omega_{3n}(t_o),$$
$$\theta_{1n}(t_f),\theta_{2n}(t_f),\theta_{3n}(t_f),\omega_{1n}(t_f),\omega_{2n}(t_f),\omega_{3n}(t_f)]^T$$
$$(n = 0,1,\ldots,N) \qquad (8.103)$$

$X_N = X_{true}$ = the true desired boundary conditions

$X_o = X_{start}$ = a set of boundary conditions for which the initial co-state variables can be determined exactly without iteration (i.e., a set of boundary conditions belonging to the sets defined by Eq. 8.88).

where $\beta_{on}(t_o)$ and $\beta_{fn}(t_f)$ are determined in terms of the sequence of 1-2-3 Euler angles θ_{1n}, θ_{2n} and θ_{3n} by the transformation of Table 2.2. Let

$$P_n = [\gamma_{0n}(t_o),\gamma_{1n}(t_o),\gamma_{2n}(t_o),\gamma_{3n}(t_o),\lambda_{1n}(t_o),\lambda_{2n}(t_o),\lambda_{3n}(t_o)]^T$$
$$= [\gamma_n^T(t_o),\lambda_n^T(t_o)]^T \quad , \quad n = 0,1,2,\ldots,N \qquad (8.104)$$

be the sequence of co-states corresponding to the solution of Eqs. 8.80 and 8.81 connecting the upper and lower partition of X_n. Initially, only the co-state P_o is known.

We introduce the continuation parameter α such that

$$0 \le \alpha_n \le 1 \quad \{0 \le \alpha_1 < \alpha_2 < \alpha_3 \ldots < \alpha_N = 1\}$$

and define the boundary conditions for the nth boundary-value problem as

$$X_n = X_o + \alpha_n[X_{true} - X_{start}] \qquad (8.105)$$

For example, set

$$\alpha_n = n/N \quad , \quad n = 0,1,\ldots,N \qquad (8.106)$$

then, clearly Eq. 8.105 satisfies the desired conditions

$$X_o = X_{start} \text{ and } X_N = X_{true} \qquad (8.107)$$

More generally, one could adjust α_n adaptively, based upon the efficiency of convergence at step n-1. In all cases, we require that Eq. 7.107 be satisfied. In the numerical example, we provide results which simply use Eq. 8.106; modifying the algorithm to make α control adaptive has not been found

necessary, but this may be due to the limited variety of maneuvers studied to date.

The starting estimate for the co-state vector (Eq. 8.104) for the nth step in the continuation process is obtained from

$$P_n = P_{n-1} + (\alpha_n - \alpha_{n-1}) \frac{dP}{d\alpha}\Big|_{n-1} \quad , \quad (n > 1) \tag{8.108}$$

where the derivative of the co-state vector with respect to the continuation parameter α is approximated via finite differences as

$$\frac{dP}{d\alpha}\Big|_{n-1} = \begin{cases} (\alpha_{n-1} - \alpha_{n-2})^{-1}\{P_{n-1} - P_{n-2}\} & , \quad (n > 1) \\ \{0\} & , \quad (n = 1) \end{cases} \tag{8.109}$$

and where P_n is the converged co-state vector for α_n (Eq. 8.104), resulting from the previous applications of the algorithm of Fig. 8.12. An accelerated quadratic estimate for the initial co-state vector (Eq. 8.109) is obtained from

$$\hat{P}_n = P_n + \Delta P_{n-1} + (\alpha_n - \alpha_{n-1}) \frac{d(\Delta P_n)}{d\alpha}\Big|_{n-1} \quad , \quad (n > 2) \tag{8.110}$$

where ΔP_n represents the actual error in the linearly predicted co-states in the nth continuation stage. The derivative of the linear co-state prediction error with respect to the continuation parameter α is approximated via finite differences as

$$\frac{d(\Delta P_n)}{d\alpha}\Big|_{n-1} = \begin{cases} (\alpha_{n-1} - \alpha_{n-2})^{-1}\{\Delta P_{n-1} - \Delta P_{n-2}\} & , \quad (n > 3) \\ \{0\} & , \quad (n \leq 2) \end{cases} \tag{8.111}$$

Each increment (controlled via specification of α_n) of the state boundary conditions (Eq. 8.106) is thus supported by a linear or better extrapolation of the co-state boundary conditions via Eq. 8.110, followed by Newton differential correction refinement using the algorithm of Fig. 8.12 (to isolate the

converged co-state P_n to desired accuracy). Observe that the process is initiated at a converged P_0 vector, and if convergence difficulties are encountered at any step of the process, one simply reduces the value of $(\alpha_n - \alpha_{n-1})$ (thereby making the error in the extrapolations, see Eqs. 8.108 or 8.110, arbitrarily small). The numerical results summarized below support the conclusion that this continuation process is not only reliable, but has also been found to be reasonably efficient.

8.5.6 An Example Maneuver

We summarize two numerical examples to illustrate the developments previously stated.

Case I is near-trivial as a numerical example, but it serves as an important validation role (since it can be rigorously solved without iteration). Case I is a "rest-to-rest" maneuver corresponding to a 90 deg reorientation about the $\hat{b}_1$ principal axis, with zero initial and final angular velocity. Table 8.4 summarizes the initial and final boundary conditions. Recognizing the Case I boundary conditions as belonging to the set I family, we calculate the following initial co-state:

$$\gamma^T(t_0) = \{0,\ -37.699118,\ 0,\ 0\}$$
$$\lambda^T(t_0) = \{-9.424778,\ 0,\ 0\} \qquad (8.112)$$

Using this initial co-state and the Case I (Table 8.4) initial state, Eq. 8.87 was integrated numerically (via a four-cycle Runge-Kutta algorithm at a constant step size of 0.01s). The numerical solution agreed at every step with the analytical solution (see Eq. 8.90) to seven digits. This test provides confidence that the formulation has been correctly coded. The control and state variables along this maneuver are sketched in Figs. 8.13a-d.

The Case II boundary conditions (Table 8.4) define a rather general "de-tumble" maneuver which is not tractable as a closed-form analytical solution. Since the vehicle is initially most nearly rotating about the $\hat{b}_1$ axis (as is

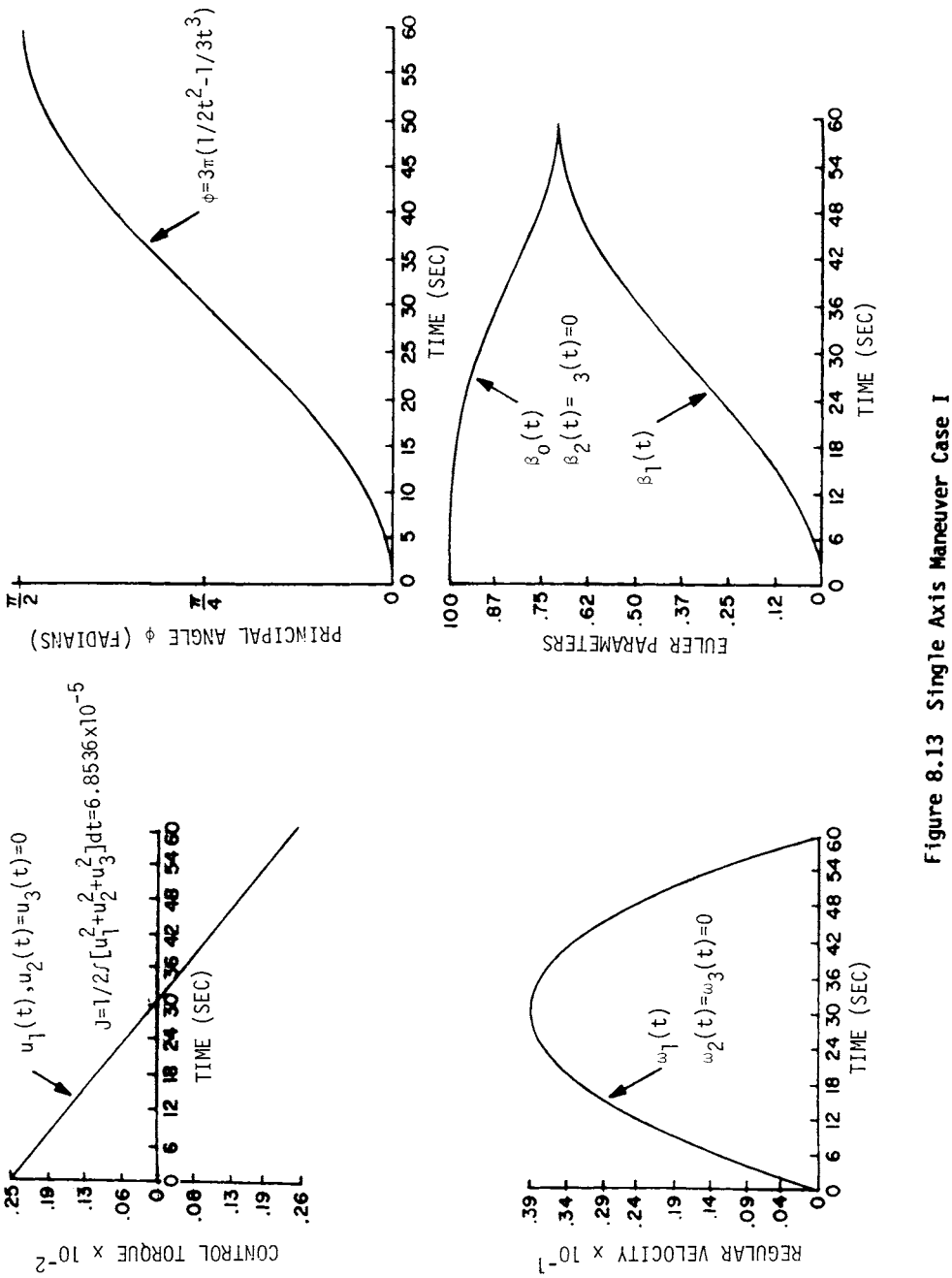

Figure 8.13 Single Axis Maneuver Case I

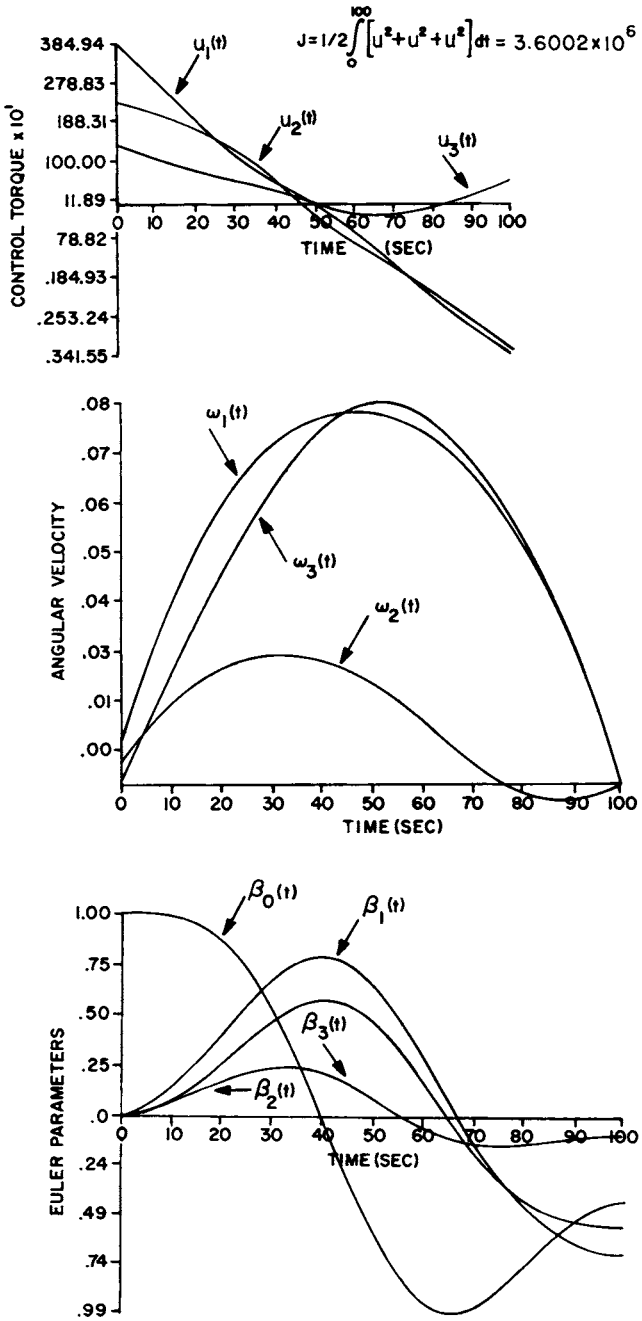

Figure 8.14 Three Axis Detumble Maneuver Case II

TABLE 8.4
ASSUMED DATA FOR CASES I AND II

	($I_1 = 1$, $I_2 = 0.8$, $I_3 = 0.5$)		(I_1=1x10^6 kg·m^2, I_2=833333 kg·m^2, I_3 = 916667 kg·m^2)	
	Initial ($t_o = 0$) state	Final (t_f = 1 min) state	Initial ($t_o = 0$) state	Final (t_f = 100 s) state
θ_1	0	$\pi/2$	0	$5\pi/2$
θ_2	0	0	0	$\pi/3$
θ_3	0	0	0	$\pi/4$
β_o	1	0.70711	1	-0.43047
β_1	0	0.70711	0	-0.70106
β_2	0	0	0	-0.09230
β_3	0	0	0	-0.56098
ω_1	0	0	0.01 rad/s	0
ω_2	0	0	0.005	0
ω_3	0	0	0.001	0

TABLE 8.5

BOUNDARY CONDITION CONTINUATION FOR CASE II

		α_n →	0	0.001	0.25	0.50	0.75	1.00
		Tolerance[a] →	...	10^{-2}	10^{-2}	10^{-2}	10^{-2}	10^{-5}
		No. of iterations →	...	1	4	6	6	4
Initial State		$\theta_1(t_o)$	0	0	0	0	0	0
		$\theta_2(t_o)$	0	0	0	0	0	0
		$\theta_3(t_o)$	0	0	0	0	0	0
		$\omega_1(t_o)$	0.01 rad/s	0.0100	0.0100	0.0100	0.0100	0.01
		$\omega_2(t_o)$	0	0.000025	0.00125	0.00250	0.00375	0.005
		$\omega_3(t_o)$	0	0.00001	0.00025	0.00050	0.00075	0.001
Final State		$\theta_1(t_f)$	$5\pi/2$	$5\pi/2$	$5\pi/2$	$5\pi/2$	$5\pi/2$	7.85397 ($\equiv 5\pi/2$)
		$\theta_2(t_f)$	0	0.01048	0.260829	0.52249	0.78471	1.04731 ($\equiv \pi/3$)
		$\theta_3(t_f)$	0	0.07857	0.19620	0.39248	0.58909	0.78546 ($\equiv \pi/4$)
		$\omega_1(t_f)$	0	0	0	0	0	0
		$\omega_2(t_f)$	0	0	0	0	0	0
		$\omega_3(t_f)$	0	0	0	0	0	0
Converged co-state ($\times 10^9$)		$\gamma_0(t_o)$	0	0	0	0	0	0
		$\gamma_1(t_o)$	-0.17649	-0.17649	-0.17685	-0.17546	-0.17082	-0.16634
		$\gamma_2(t_o)$	0	-0.00063	-0.01501	-0.02674	-0.03496	-0.04117
		$\gamma_3(t_o)$	0	-0.00039	-0.01101	-0.02672	-0.04411	-0.05838
		$\lambda_1(t_o)$	-4.3124	-4.31237	-4.22029	-4.01835	-3.81454	-3.64945
		$\lambda_2(t_o)$	0	-0.01576	-0.37601	-0.67991	-0.91423	-1.10589
		$\lambda_3(t_o)$	0	-0.03034	-0.73721	-1.34988	-1.80119	-2.13870

[a]Maximum relative error in ω's (normalized by 0.001), and β's (normalized by 1).

evidenced by the relative magnitude of the initial ω_i's), the decision is made to use initial and final boundary conditions corresponding to pure spin about $\hat{\mathbf{b}}_1$ to start the continuation process of Section 8.5.5. Table 8.5 lists the sequence of boundary-value settings and converged co-states resulting from the continuation process. In this particular case, we took N=5 in Eq. 8.106 and we found most reliable and efficient convergence ensued using the differential correction algorithm of Fig. 8.12. For each of the five continuation steps, an average of four differential corrections were required. The rigorous partial derivatives of the state transition matrix were computed and used for the first differential correction for each continuation-step, with approximate partial derivatives being generated for successive differential corrections by the method of Reference 18. The final optimal maneuver, which converged to seven digits, is sketched in Figs. 8.14a-c. This example appears to be of representative difficulty; the unqualified successful determination of this optimal maneuver (and several parameter variations thereof) provides the basis for our guarded optimism. We believe that this approach will converge for a very broad family of maneuvers.

In a recent paper [20], we show an alternative, more elegant and efficient way to compute the initial co-state vector which accomplishes the minimization of Eq. 8.98. In addition, we establish that the co-state vector, if normalized by B, are themselves a set of Euler parameters defining the instantaneous orientation of $\{\hat{\mathbf{b}}\}$ relative to a displaced inertial frame. We believe the above results should be studied in conjunction with Ref. [20] to gain a full appreciation for this problem.

8.6 CONCLUDING REMARKS

This chapter demonstrates a rich variety of nonlinear optimal maneuvers of rigid and multiple rigid body spacecraft. For many applications these *open loop controls* must be supplemented by *feedback controls* to compensate for

model errors, actuation errors, and external disturbances. For some applications (e.g. the magnetic attitude maneuvers of the NOVA spacecraft, Ref. 19), these open loop maneuvers can be directly implemented without feedback.

REFERENCES

1. Tossman, B. E., "A Time Optimal Geomagnetic Maneuvering Technique for Orbit Correction Thrust Vectoring," **Proceedings of the 12th International Symposium on Space Technology and Science** (Tokyo, 1977), Pergamon Press, New York, 1977, pp. 389-398.

2. Tossman, B. E., "Magnetic Attitude Control System for the Radio Astronomy Explorer-A Satellite," **Journal of Spacecraft and Rockets**, Vol. 6, March 1969, pp. 239-244.

3. Shiegehara, M., "Geomagnetic Attitude Control of an Axisymmetric Spinning Satellite," **Journal of Spacecraft and Rockets**, Vol. 9, June 1972, pp. 391-398.

4. Kershner, R. B. and Newton, R. R., "The TRANSIT System," **Journal of the Institute of Navigation**, Vol. 15, 1962, pp. 129-144.

5. Grasshoff, L. H., "A Method for Controlling the Attitude of a Spin-Stabilized Satellite," **ARS Journal**, Vol. 31, May 1961, pp. 646-649.

6. Renard, M. L., "Command Laws for Magnetic Attitude Control of Spin-Stabilized Earth Satellites," **Journal of Spacecraft and Rockets**, Vol.4 , Feb. 1967, pp. 156-163.

7. Sorensen, J. A., "A Magnetic Attitude Control System for an Axisymmetric Spinning Spacecraft," **Journal of Spacecraft and Rockets**, Vol. 8, May 1971, pp. 441-448.

8. Rajaram, S. and Goel, P. S., "Magnetic Attitude Control of Near Earth Spinning Satellites," **Journal of the British Interplanetary Society**, Vol. 31, 1978, pp. 163-167.

9. Goel, P. S. and Rajaram, S., "Magnetic Attitude Control of a Momentum-Biased Satellite in Near-Equatorial Orbit," **Journal of Guidance and Control**, Vol. 2, July-Aug. 1979, pp. 334-338.

10. Alfriend, K. T., "Magnetic Attitude Control System for Dual-Spin Satellites," **AIAA Journal**, Vol. 13, June 1975, pp. 817-822.

11. Stickler, A. C. and Alfriend, K. T., "Elementary Magnetic Attitude Control System," **Journal of Spacecraft and Rockets**, Vol. 13, May 1976, pp. 282-287.

12. Takezawa, S. and Ninomiya, K., "A New Approach to the Analysis and Design of Magnetic Stabilization of Satellites," **Proceedings of the 30th Congress of the IAF**, Paper IAF-79-106, Pergamon Press, New York, Sept. 1979.

13. Junkins, J. L., Carrington, C. K., and Williams, C. E., "Time-Optimal Magnetic Attitude Maneuvers," **AIAA Journal of Guidance and Control**, Vol. 4, No. 4, pp. 363-368, 1981.

14. Strumanis, M., "Geomagnetic Field Model," an IBM 360 Library Program Documentation of BMAG, The Johns Hopkins Applied Physics Lab, Laurel, Md., Dec. 1968.

15. Vadali, S. R., and Junkins, J. L., "Spacecraft Large Angle Rotational Maneuvers with Optimal Momentum Transfer," Presented to the AIAA Astrodynamics Conference, San Diego, CA, August 1982.

16. Junkins, J. L., and Turner, J. D., "Optimal Continuous Torque Attitude Maneuvers," **AIAA Journal of Guidance and Control**, Vol. 3, pp. 210-217, May-June 1980.

17. Junkins, J. L. and Turner, J. D., "Optimal Continuous Torque Attitude Maneuvers," Paper 78-1400, AIAA/AAS Astrodynamics Conference, Palo Alto, Calif., Aug. 7-9, 1978.

18. Junkins, J. L., "On the Determination and Optimization of Powered Space Trajectories Using Parameteric Differential Correction Processes," McDonnell Douglas Rept. 61793, Huntington Beach, Calif., Dec. 1969.

19. Utterback, H. K., et al., "NOVA INFORMATION PROCESSING SYSTEM," The Johns Hopkins Applied Physics Laboratory Report # SDO-5511, Laurel, MD., Rev. March, 1981.

20. Vadali, S. R., Kraige, L. G., and Junkins, J. L., "New Results on the Optimal Spacecraft Attitude Maneuver Problem," **AIAA Journal of Guidance and Control**, Vol. 7, No. 3, pp. 378-380, May-June 1984.